Exploring Strong Field Gravity

Christopher Berry

Churchill College
and
Institute of Astronomy,
University of Cambridge

Supervisor: Jonathan Gair

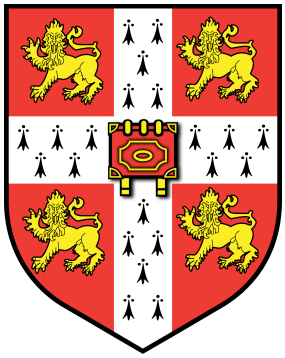

Certificate of Postgraduate Study

6 July 2010

Abstract

Abstract

Chapter 1

Introduction

1.1 Introduction

'Lo

1.2 Conventions

Throughout this work we will use the the time-like sign convention of Landau and Lifshitz[1]:

1. The metric has signature $(+,-,-,-)$.
2. The Reinann tensor is defined as $R^{\mu}{}_{\nu\sigma\rho} = \partial_{\sigma}\Gamma^{\mu}{}_{\nu\rho} - \partial_{\rho}\Gamma^{\mu}{}_{\nu\sigma} + \Gamma^{\mu}{}_{\lambda\sigma}\Gamma^{\lambda}{}_{\rho\nu} - \Gamma^{\mu}{}_{\lambda\rho}\Gamma^{\lambda}{}_{\sigma\nu}$.
3. The Ricci tensor is defined as the contraction $R_{\mu\nu} = R^{\lambda}{}_{\mu\lambda\mu}$.

Greek indices are used to represent spacetime indices $\mu = \{0,1,2,3\}$ and lowercase Latin indices from the middle of the alphabet are used for spatial indices $i = \{1,2,3\}$. Uppercase Latin indices from the beginning of the alphabet will be used for the output of two LISA detector arms $A = \{\mathrm{I},\mathrm{II}\}$, and lowercase Latin indices from the beginning of the alphabet are used for parameter space. Summation over repeated indices is assumed unless explicitly noted otherwise. Geometric units with $G = c = 1$ will be used where noted, but in general factors of G and c will be retained.

Chapter 2

Gravitational Radiation In $f(R)$ Theory

2.1 Introduction To $f(R)$ Theory

General relativity (GR) is a well tested theory of gravity [2], however it is still interesting to explore alternate theories. This may be motivated by the need to explain dark matter and dark matter in cosmology, trying to formulate a quantizable theory of gravity or simple curiosity regarding the uniqueness of GR. One of the simplest extensions to standard GR are the class of $f(R)$ theories [3, 4].

2.1.1 The Action & Field Equations

General relativity may be derived from the Einstein-Hilbert action [1, 5]

$$S_{\mathrm{EH}}[g] = \frac{c^4}{16\pi G}\int R\sqrt{-g}\,\mathrm{d}^4x. \tag{2.1}$$

In $f(R)$ theory we make a simple modification of the action to include an arbitrary function of the Ricci scalar R such that [6]

$$S[g] = \frac{c^4}{16\pi G}\int f(R)\sqrt{-g}\,\mathrm{d}^4x. \tag{2.2}$$

We will assume that $f(R)$ is analytic about $R = 0$ so that it may be expressed as a power series [7]

$$f(R) = a_0 + a_1R + \frac{a_2}{2!}R^2 + \frac{a_3}{3!}R^3 + \dots \tag{2.3}$$

Note that since the dimensions of $f(R)$ must be the same as of R, $[a_n] = [R]^{(1-n)}$. To link to GR we will set $a_1 = 1$; any rescaling may be absorbed into the definition of G.

The field equations are obtained by a variational principle; there are a number of choice for achieving this. To derive the Einstein field equations from the Einstein-Hilbert action one may use the standard metric variation or the Palatini variation [5]. Both approaches may be used for $f(R)$, however they now yield different results [3, 4].

Following the metric (or second order) formalism, one varies the action with respect to the metric $g^{\mu\nu}$, the resulting field equations are those for metric $f(R)$ gravity. Following the Palantini (or first order) formalism one varies the action with respect both to the metric $g^{\mu\nu}$ and to the connection $\Gamma^{\rho}{}_{\mu\nu}$, which are treated as independent quantities: the connection is not the Levi-Cevita metric connection.[1]

Finally, there is a third version of $f(R)$ gravity: metric-affine $f(R)$ gravity.

Varying the action with respect to the metric $g^{\mu\nu}$ produces

$$\delta S = \frac{c^4}{16\pi G}\int\left\{f'(R)\sqrt{-g}\left[R_{\mu\nu} - \nabla_\mu\nabla_\nu \ + g_{\mu\nu}\Box\right] - f(R)\frac{1}{2\sqrt{-g}}g g_{\mu\nu}\right\}\delta g^{\mu\nu}\,\mathrm{d}^4x, \quad (2.4)$$

where $\Box - g^{\mu\nu}\nabla_\mu\nabla_\nu$ is the d'Alembertian and a prime denotes differentiation with respect to R. Proceeding from here certain assumptions regarding surface terms.

Integrating by parts and assuming that the variation $\delta g^{\mu\nu}$ vanishes at infinity allows this to be rewritten as

$$\delta S = \frac{c^4}{16\pi G}\int\left\{f'(R)R_{\mu\nu} - \nabla_\mu\nabla_\nu f'(R) + g_{\mu\nu}\Box f'(R) - f(R)\frac{1}{2}g_{\mu\nu}\right\}\delta g^{\mu\nu}\sqrt{-g}\,\mathrm{d}^4x. \quad (2.5)$$

For the action to be extremised for, $\delta S = 0$, for any variation $\delta g^{\mu\nu}$, the term in braces must vanish.

Thus we obtain the vacuum field equation

$$f'R_{\mu\nu} - \nabla_\mu\nabla_\nu f' + g_{\mu\nu}\Box f' - \frac{f}{2}g_{\mu\nu} = 0. \quad (2.6)$$

For standard GR, when $f(R) = R$, this reduces to the familiar

$$R_{\mu\nu} - \frac{R}{2}g_{\mu\nu} = 0. \quad (2.7)$$

Taking the trace of our field equation gives

$$f'R + 3\Box f' - 2f = 0. \quad (2.8)$$

Note if we consider a uniform flat spacetime $R = 0$, this equation gives

$$a_0 = 0. \quad (2.9)$$

In analogy to the Einstein tensor, we shall define

$$\mathcal{G}_{\mu\nu} = f'R_{\mu\nu} - \nabla_\mu\nabla_\nu f' + g_{\mu\nu}\Box f' - \frac{f}{2}g_{\mu\nu}, \quad (2.10)$$

so that in a vacuum

$$\mathcal{G}_{\mu\nu} = 0. \quad (2.11)$$

[1] Imposing that the metric and Palantini formalisms produce the same field equations, for an action that only depends on the metric and Reimann tensor, selects Lovelock gravity [8]. GR is a special case of Lovelock gravity; $f(R)$ gravity only coincides with Lovelock gravity when it reduces back to GR (with or without a cosmological constant).

2.1.2 Conservation Of Energy-Momentum

If we introduce matter with a stress-energy tensor $T_{\mu\nu}$, the field equation becomes

$$\mathcal{G}_{\mu\nu} = \frac{8\pi G}{c^4} T_{\mu\nu}. \tag{2.12}$$

If we act upon this with the covariant derivative we obtain

$$\begin{aligned} \frac{8\pi G}{c^4}\nabla^\mu T_{\mu\nu} &= \nabla^\mu \mathcal{G}_{\mu\nu} \\ &= R_{\mu\nu}\nabla^\mu f' + f'\nabla^\mu\left(R_{\mu\nu} - \frac{1}{2}Rg_{\mu\nu}\right) - \left(\Box\nabla_\nu - \nabla_\nu\Box\right) f'. \end{aligned} \tag{2.13}$$

The second term contains the covariant derivative of the Einstein tensor and so is zero. After some manipulation the final term can be shown to be

$$\begin{aligned} \left(\Box\nabla_\nu - \nabla_\nu\Box\right) f' &= g^{\mu\sigma}\left[\nabla_\mu\nabla_\sigma\nabla_\nu - \nabla_\nu\nabla_\mu\nabla_\sigma\right] f' \\ &= R_{\tau\nu}\nabla^\tau f', \end{aligned} \tag{2.14}$$

which is a useful geometric identity. Using this we find that

$$\begin{aligned} \frac{8\pi G}{c^4}\nabla^\mu T_{\mu\nu} &= R_{\mu\nu}\nabla^\mu f' - R_{\mu\nu}\nabla^\mu f' \\ &= 0. \end{aligned} \tag{2.15}$$

Consequently we see that energy-momentum is a conserved quantity in the same way as in GR, as may be expected from the symmetries of the action.

2.2 Linear Perturbations

We will now consider the case that the metric is perturbed slightly from flat Minkowski such that

$$g_{\mu\nu} = \eta_{\mu\nu} + h_{\mu\nu}, \tag{2.16}$$

where more formally we mean that $h_{\mu\nu} = \epsilon H_{\mu\nu}$ for small parameter ϵ. We will consider terms only to $\mathcal{O}(\epsilon)$. Thus, the inverse metric is

$$g^{\mu\nu} = \eta^{\mu\nu} - h^{\mu\nu}, \tag{2.17}$$

where we have used the Minkowski metric to raise the indices on the right side, effectively defining

$$h^{\mu\nu} = \eta^{\mu\sigma}\eta^{\nu\rho}h_{\sigma\rho}. \tag{2.18}$$

Similarly, the trace h is given by

$$h = \eta^{\mu\nu}h_{\mu\nu}. \tag{2.19}$$

This means that all quantities denoted by "h" are strictly $\mathcal{O}(\epsilon)$. We will have to be careful later on to distinguish between quantities where the Minkowski metric has been used to raise indices and those where the full metric has been used.

The linearized ($\mathcal{O}(\epsilon)$) connection coefficient is

$$\Gamma^{(1)\rho}{}_{\mu\nu} = \frac{1}{2}\eta^{\rho\lambda}(\partial_\mu h_{\lambda\nu} + \partial_\nu h_{\lambda\mu} - \partial_\lambda h_{\mu\nu}). \tag{2.20}$$

The covariant derivative of any perturbed quantity will be the same as the partial derivative. The Riemann tensor is

$$R^{(1)\lambda}{}_{\mu\nu\rho} = \frac{1}{2}(\partial_\mu\partial_\nu h^\lambda_\rho + \partial^\lambda\partial_\rho h_{\mu\nu} - \partial_\mu\partial_\rho h^\lambda_\nu - \partial^\lambda\partial_\nu h_{\mu\rho}), \tag{2.21}$$

where we have raised the index on the differential operator with the background Minkowski metric. Contracting gives the Ricci tensor

$$R^{(1)}{}_{\mu\nu} = \frac{1}{2}(\partial_\mu\partial_\rho h^\rho_\nu + \partial_\nu\partial_\rho h^\rho_\mu - \Box h_{\mu\nu} - \partial_\mu\partial_\nu h), \tag{2.22}$$

where the d'Alembertian operator is $\Box = \eta^{\mu\nu}\partial_\mu\partial_\nu$. Contracting this with $\eta^{\mu\nu}$ we find the first order Ricci scalar

$$R^{(1)} = \partial_\mu\partial_\rho h^{\rho\mu} - \Box h. \tag{2.23}$$

Since $R^{(1)}$ is $\mathcal{O}(\epsilon)$ we may write $f(R)$ as a Maclaurin series to first order such that

$$f^{(1)}(R) = a_0 + R^{(1)} \tag{2.24}$$

$$f'^{(1)}(R) = 1 + a_2 R^{(1)}. \tag{2.25}$$

As we are perturbing from a flat Minkowski background where the Ricci scalar vanishes, we may use equation (2.9) to set $a_0 = 0$. Inserting these into equation (2.6) and retaining terms to first order we obtain

$$R^{(1)}{}_{\mu\nu} - \partial_\mu\partial_\nu(a_2 R^{(1)}) + \eta_{\mu\nu}\Box(a_2 R^{(1)}) - \frac{R^{(1)}}{2}\eta_{\mu\nu} = 0. \tag{2.26}$$

We see that we need to find a relation between $R^{(1)}$ and its derivatives. Let us consider the linearized equation (2.8)

$$\begin{aligned} R^{(1)} + 3\Box(a_2 R^{(1)}) - 2R^{(1)} &= 0 \\ 3a_2\Box R^{(1)} - R^{(1)} &= 0 \end{aligned} \tag{2.27}$$

This is the massive Klein-Gordon equation

$$\Box R^{(1)} + m^2 R^{(1)} = 0, \tag{2.28}$$

if we define mass

$$m^2 = -\frac{1}{3a_2}. \tag{2.29}$$

For a physically meaningful solution we require $m^2 > 0$, thus we constrain $f(R)$ such that $a_2 < 0$.[2] Now substituting for $\Box R^{(1)}$ in the field equation gives

$$\begin{aligned} R^{(1)}{}_{\mu\nu} - a_2\partial_\mu\partial_\nu R^{(1)} + \frac{R^{(1)}}{3}\eta_{\mu\nu} - \frac{R^{(1)}}{2}\eta_{\mu\nu} &= 0 \\ R^{(1)}{}_{\mu\nu} - a_2\partial_\mu\partial_\nu R^{(1)} - \frac{R^{(1)}}{6}\eta_{\mu\nu} &= 0. \end{aligned} \tag{2.30}$$

[2] Use of the other sign convention for the metric would result in the reversal of this inequality.

The next step is to substitute in $h_{\mu\nu}$ to try to find wave solutions. We hope to find a quantity $\overline{h}_{\mu\nu}$ that will satisfy a wave equation, where it is related to $h_{\mu\nu}$ by

$$\overline{h}_{\mu\nu} = h_{\mu\nu} + A_{\mu\nu}. \tag{2.31}$$

In GR we use the trace reversed form where $A_{\mu\nu} = -(h/2)\eta_{\mu\nu}$. This will not suffice here as we have additional terms, but let us look for a similar solution

$$\overline{h}_{\mu\nu} = h_{\mu\nu} - \frac{h}{2}\eta_{\mu\nu} + B_{\mu\nu}. \tag{2.32}$$

The only rank two tensors in our theory are: $h_{\mu\nu}$, $\eta_{\mu\nu}$, $R_{\mu\nu}$, and $\partial_\mu\partial_\nu$; $h_{\mu\nu}$ has been used already, and we wish to eliminate $R_{\mu\nu}$, so we will try the simpler option based around $\eta_{\mu\nu}$. We want $B_{\mu\nu}$ to be $\mathcal{O}(\epsilon)$. There are three scalar quantities that satisfy this: h, R and $\Box R$; h is used already and $\Box R$ is related to R by equation (2.27). Therefore, we may construct an ansatz

$$\overline{h}_{\mu\nu} = h_{\mu\nu} + \left(ba_2R - \frac{h}{2}\right)\eta_{\mu\nu} \tag{2.33}$$

where a_2 has been included to ensure dimensional consistency, and b is a dimensionless number. Contracting with the background metric yields

$$\overline{h} = 4ba_2R - h, \tag{2.34}$$

so we may eliminate h in our definition of $\overline{h}_{\mu\nu}$ to give

$$h_{\mu\nu} = \overline{h}_{\mu\nu} + \left(ba_2R - \frac{\overline{h}}{2}\right)\eta_{\mu\nu}. \tag{2.35}$$

We will assume a Lorenz, or de Donder, gauge choice such that

$$\nabla^\mu\overline{h}_{\mu\nu} = 0, \tag{2.36}$$

to first order this gives

$$\partial^\mu\overline{h}_{\mu\nu} = 0. \tag{2.37}$$

Subject to this, the Ricci tensor is, from equation (2.22),

$$\begin{aligned} R_{\mu\nu} = \frac{1}{2}\Bigg\{&\partial_\nu\partial_\mu\left(ba_2R - \frac{\overline{h}}{2}\right) + \partial_\mu\partial_\nu\left(ba_2R - \frac{\overline{h}}{2}\right) \\ &-\Box\left[\overline{h}_{\mu\nu} + \left(ba_2R - \frac{\overline{h}}{2}\right)\eta_{\mu\nu}\right] - \partial_\mu\partial_\nu(4ba_2R - \overline{h})\Bigg\} \\ = -\frac{1}{2}&\left\{2ba_2\partial_\mu\partial_\nu R + \Box\left(\overline{h}_{\mu\nu} - \frac{\overline{h}}{2}\eta_{\mu\nu}\right) + \frac{b}{3}R\eta_{\mu\nu}\right\}. \end{aligned} \tag{2.38}$$

Using this in our field equation (2.30) gives

$$\frac{1}{2}\Box\left(\overline{h}_{\mu\nu} - \frac{\overline{h}}{2}\right) + (b+1)\left(a_2\partial_\mu\partial_\nu R + \frac{R}{6}\eta_{\mu\nu}\right) = 0. \tag{2.39}$$

If we set $b = -1$, then the second term vanishes. Let us now consider the Ricci scalar in the case $b = -1$, then from equation (2.23)

$$\begin{aligned} R &= \Box\left(a_2 R - \frac{\overline{h}}{2}\right) - \Box(-4a_2 R - \overline{h}) \\ &= 3a_2\Box R + \frac{1}{2}\Box\overline{h}. \end{aligned} \tag{2.40}$$

For consistency with equation (2.27), we see that

$$\Box\overline{h} = 0. \tag{2.41}$$

This means finally that

$$\Box\overline{h}_{\mu\nu} = 0, \tag{2.42}$$

we have our wave equation and it is consistent.

Should a_2 be sufficiently small that it may be regarded an $\mathcal{O}(\epsilon)$ quantity, we recover GR to leading order within our analysis.

2.3 Gravitational Radiation

Having established two wave equations, (2.27) and (2.42), we may now investigate their solutions. We will use natural units $c = \hbar = 1$. Using a standard Fourier decomposition

$$\overline{h}_{\mu\nu} = \Re\left\{\widehat{\overline{h}}_{\mu\nu}(k_\rho)\exp\left(ik_\rho x^\rho\right)\right\}, \tag{2.43}$$

$$R = \Re\left\{\widehat{R}(q_\rho)\exp\left(iq_\rho x^\rho\right)\right\}, \tag{2.44}$$

where k_μ and q_μ are the 4-wavevectors, or 4-momenta, of the waves. From equation (2.42) we know that k_μ is a null vector, so for a wave travelling along the z-axis

$$k^\mu = \omega(1, 0, 0, 1), \tag{2.45}$$

where ω is the frequency. Similarly, from equation (2.27)

$$q^\mu = (\Omega, 0, 0, \sqrt{\Omega^2 - m^2}), \tag{2.46}$$

for frequency Ω. This means that these waves do not travel at c, but have a group velocity

$$v = \frac{\sqrt{\Omega^2 - m^2}}{\Omega}. \tag{2.47}$$

Provided that $m^2 > 0$, $v < c = 1$, but we do not get propagating modes for $\Omega^2 < m^2$.

From the condition (2.36) we find that k^μ is orthogonal to $\widehat{\overline{h}}_{\mu\nu}$,

$$k^\mu\widehat{\overline{h}}_{\mu\nu} = 0, \tag{2.48}$$

thus in this case

$$\widehat{\overline{h}}_{0\nu} + \widehat{\overline{h}}_{3\nu} = 0. \tag{2.49}$$

Let us now consider the implications of equation (2.41) using equations (2.34) and (2.27),

$$\begin{aligned} \Box\left(4a_2R + h\right) &= 0 \\ \Box h &= -\frac{4}{3}R. \end{aligned} \tag{2.50}$$

For non-zero R (as required for the Ricci mode) there is no way we can make such that the trace h will vanish. This is distinct from the case in GR. It is possible, however, to make a gauge choice such that the trace $\overline{h}$ will vanish. Consider a gauge transformation generated by ξ_μ which satisfies $\Box\xi_\mu = 0$, and so has a Fourier decomposition

$$\xi_\mu = \widehat{\xi}_\mu \exp\left(ik_\rho x^\rho\right). \tag{2.51}$$

We see that a transformation

$$\overline{h}_{\mu\nu} \to \overline{h}_{\mu\nu} + \partial_\mu\xi_\nu + \partial_\nu\xi_\mu - \eta_{\mu\nu}\partial^\rho\xi_\rho, \tag{2.52}$$

would ensure both conditions (2.36) and (2.42) are satisfied. Under such a transformation

$$\widehat{\overline{h}}_{\mu\nu} \to \widehat{\overline{h}}_{\mu\nu} + i\left(k_\mu\widehat{\xi}_\nu + k_\nu\widehat{\xi}_\mu - \eta_{\mu\nu}k^\rho\widehat{\xi}_\rho\right). \tag{2.53}$$

We may therefore impose four further constraints (one for each $\widehat{\xi}_\mu$) upon $\widehat{\overline{h}}_{\mu\nu}$, and we may take these to be

$$\widehat{\overline{h}}_{0\nu} = 0, \quad \widehat{\overline{h}} = 0. \tag{2.54}$$

This may appear to be five constraints, however we have already imposed (2.49), and so setting $\widehat{\overline{h}}_{00} = 0$ automatically implies $\widehat{\overline{h}}_{03} = 0$.

We see that $\overline{h}_{\mu\nu}$ behaves just as its counterpart in GR so we may define

$$\left[\widehat{\overline{h}}_{\mu\nu}\right] = \begin{bmatrix} 0 & 0 & 0 & 0 \\ 0 & h_+ & h_\times & 0 \\ 0 & h_\times & -h_+ & 0 \\ 0 & 0 & 0 & 0 \end{bmatrix}, \tag{2.55}$$

where h_+ and $h_\times$ are appropriate constants representing the amplitudes of the two transverse polarizations of gravitational radiation.

Using this choice of gauge we have

$$h_{\mu\nu} = \overline{h}_{\mu\nu} - a_2R\eta_{\mu\nu}, \tag{2.56}$$

$$h = -4a_2R. \tag{2.57}$$

Combining both wave modes ($\overline{h}_{\mu\nu}$ and R) the perturbation to the flat background associated with our wave solutions looks like

$$[h_{\mu\nu}(z,t)] = \begin{bmatrix} -a_2\widehat{R}(t-vz) & 0 & 0 & 0 \\ 0 & h_+(t-z) + a_2\widehat{R}(t-vz) & h_\times(t-z) & 0 \\ 0 & h_\times(t-z) & -h_+ + a_2\widehat{R}(t-vz) & 0 \\ 0 & 0 & 0 & a_2\widehat{R}(t-vz) \end{bmatrix}. \tag{2.58}$$

If we now assume that both are excited by the same source so that the frequencies will be equal $\omega = \Omega$.

It is important that our solutions reduce to those of GR in the event that $f(R) = R$. In this linearized approach this corresponds to $a_2 \to 0$, $m^2 \to \infty$. We see from equation (2.46) that in this limit it would take an infinite frequency to excite a propagating Ricci mode, and evanescent waves would decay away infinitely quickly. Therefore there would not be any detectable Ricci modes and we would only observe the two polarizations found in the analysis of GR. Additionally $\overline{h}_{\mu\nu}$ would simplify to its usual trace-reversed form.

2.4 Energy-momentum Tensor

We expect that the gravitational field would carry energy-momentum. Unfortunately it is difficult to define a proper energy-momentum tensor for a gravitational field: as a consequence of the equivalence principle it is possible to transform to a freely falling frame, eliminating the gravitational field and any associated energy density for a given event, although we may still define curvature in the neighbourhood of this point. We see that the full field equation, equation (2.6), has no energy-momentum tensor for the gravitational field on the right-hand side. However, by expanding beyond the linear terms we may find a suitable energy-momentum pseudotensor for gravitational radiation. We may expand $\mathcal{G}_{\mu\nu}$ in orders of $h_{\mu\nu}$

$$\mathcal{G}_{\mu\nu} = \mathcal{G}^{(\mathrm{B})}{}_{\mu\nu} + \mathcal{G}^{(1)}{}_{\mu\nu} + \mathcal{G}^{(2)}{}_{\mu\nu} + \dots \tag{2.59}$$

We use (B) for the background term instead of (0) to avoid confusion regarding its order in ϵ. Our linearised equation would then read

$$\mathcal{G}^{(1)}{}_{\mu\nu} = 0. \tag{2.60}$$

So far we have assumed that our background is flat, however we can imagine that should the gravitational radiation carry energy-momentum then this would act as a source of curvature for the background. This is a second-order effect that may be encoded, to accuracy of $\mathcal{O}(\epsilon^2)$, as

$$\mathcal{G}^{(\mathrm{B})}{}_{\mu\nu} = -\mathcal{G}^{(2)}{}_{\mu\nu}. \tag{2.61}$$

By shifting $\mathcal{G}^{(2)}{}_{\mu\nu}$ to the right-hand side we effectively create an energy-momentum tensor. As in GR we will average over several wavelengths, assuming that the background curvature is on a larger scale,

$$\mathcal{G}^{(\mathrm{B})}{}_{\mu\nu} = -\left\langle \mathcal{G}^{(2)}{}_{\mu\nu} \right\rangle. \tag{2.62}$$

By doing this, we may probe the curvature in a macroscopic region about a given point in spacetime. This gives a gauge invariant measure of the gravitational field strength. The averaging can be thought of as smoothing out the rapidly varying ripples of the radiation, leaving only the coarse-grained component that acts as a source for the background curvature. The energy-momentum pseudotensor for the radiation may be identified as

$$t_{\mu\nu} = -\frac{c^4}{8\pi G}\left\langle \mathcal{G}^{(2)}{}_{\mu\nu} \right\rangle. \tag{2.63}$$

Having made this provisional identification, we must now set about carefully evaluating the various terms in equation (2.59). We begin as in section 2.2 by defining a total metric

$$g_{\mu\nu} = \gamma_{\mu\nu} + h_{\mu\nu}, \tag{2.64}$$

where $\gamma_{\mu\nu}$ is our background metric. This is changing slightly our definition for $h_{\mu\nu}$: instead of it being the total perturbation from flat Minkowski, it is instead the dynamical part of the metric with which we associate radiative effects. Since we know that ${\mathcal{G}^{(\mathrm{B})}}_{\mu\nu}$ is $\mathcal{O}(\epsilon^2)$, we may decompose our background metric as

$$\gamma_{\mu\nu} = \eta_{\mu\nu} + j_{\mu\nu}, \tag{2.65}$$

where $j_{\mu\nu}$ is $\mathcal{O}(\epsilon^2)$ to ensure that ${R^{(\mathrm{B})\lambda}}_{\mu\nu\rho}$ is also $\mathcal{O}(\epsilon^2)$. Therefore its introduction will make no difference to the linearized theory.

We will consider terms only to $\mathcal{O}(\epsilon^2)$. The connection coefficient is

$${\Gamma^{\rho}}_{\mu\nu} = {\Gamma^{(\mathrm{B})\rho}}_{\mu\nu} + {\Gamma^{(1)\rho}}_{\mu\nu} + {\Gamma^{(2)\rho}}_{\mu\nu} + \ldots \tag{2.66}$$

We identify ${\Gamma^{(1)\rho}}_{\mu\nu}$ from equation (2.20) to the accuracy of our analysis. There is one small subtlety: whether we use the background metric $\gamma^{\mu\nu}$ or $\eta^{\mu\nu}$ to raise indices of ∂_μ and $h_{\mu\nu}$. Fortunately, to the accuracy considered here, it does not make a difference; however, we will consider the indices to be changed with the background metric. This is more appropriate for considering the effect of curvature on gravitational radiation. We will not distinguish between ∂_μ and ${\nabla^{(\mathrm{B})}}_\mu$, the covariant derivative for the background metric: note that to the order of accuracy considered here covariant derivatives would commute and ${\nabla^{(\mathrm{B})}}_\mu$ behaves just like ∂_μ. The connection coefficient has

$$\begin{aligned}{\Gamma^{(1)\rho}}_{\mu\nu} = \frac{1}{2}\gamma^{\rho\lambda}\Big[&\partial_\mu\left(\overline{h}_{\lambda\nu} - a_2 R^{(1)}\gamma_{\lambda\nu}\right) + \partial_\nu\left(\overline{h}_{\lambda\mu} - a_2 R^{(1)}\gamma_{\lambda\mu}\right) \\ &- \partial_\lambda\left(\overline{h}_{\mu\nu} - a_2 R^{(1)}\gamma_{\mu\nu}\right)\Big],\end{aligned} \tag{2.67}$$

where $R^{(1)}$ is the first order Ricci scalar, and

$$\begin{aligned}{\Gamma^{(2)\rho}}_{\mu\nu} =& -\frac{1}{2}h^{\rho\lambda}(\partial_\mu h_{\lambda\nu} + \partial_\nu h_{\lambda\mu} - \partial_\lambda h_{\mu\nu}) \\ =& -\frac{1}{2}\left(\overline{h}^{\rho\lambda} - a_2 R^{(1)}\gamma^{\rho\lambda}\right)\Big[\partial_\mu\left(\overline{h}_{\lambda\nu} - a_2 R^{(1)}\gamma_{\lambda\nu}\right) + \partial_\nu\left(\overline{h}_{\lambda\mu} - a_2 R^{(1)}\gamma_{\lambda\mu}\right) \\ &- \partial_\lambda\left(\overline{h}_{\mu\nu} - a_2 R^{(1)}\gamma_{\mu\nu}\right)\Big].\end{aligned} \tag{2.68}$$

The Riemann tensor is

$${R^{\lambda}}_{\mu\nu\rho} = {R^{(\mathrm{B})\lambda}}_{\mu\nu\rho} + {R^{(1)\lambda}}_{\mu\nu\rho} + {R^{(2)\lambda}}_{\mu\nu\rho} + \ldots \tag{2.69}$$

We may use our expression from equation (2.21) for ${R^{(1)\lambda}}_{\mu\nu\rho}$. Contracting gives the Ricci tensor

$$R_{\mu\nu} = {R^{(\mathrm{B})}}_{\mu\nu} + {R^{(1)}}_{\mu\nu} + {R^{(2)}}_{\mu\nu} + \ldots \tag{2.70}$$

We may again use our linearized expression, equation (2.22), for the first order term.

$$\begin{aligned} {R^{(1)}}_{\mu\nu} &= \frac{1}{2}\Big[\partial_\mu\partial_\rho\left(\overline{h}^\rho_\nu - a_2 R^{(1)}\gamma^\rho_\nu\right) + \partial_\nu\partial_\rho\left(\overline{h}^\rho_\mu - a_2 R^{(1)}\gamma^\rho_\mu\right) \\ &\quad - \Box^{(\mathrm{B})}\left(\overline{h}_{\mu\nu} - a_2 R^{(1)}\gamma_{\mu\nu}\right) - \partial_\mu\partial_\nu\left(-4a_2 R\right)\Big] \\ &= 2a_2\partial_\mu\partial_\nu R^{(1)} + \frac{1}{6}R^{(1)}\gamma_{\mu\nu}, \end{aligned} \tag{2.71}$$

Note that the d'Almebertian is now $\Box^{(\mathrm{B})} = \gamma^{\mu\nu}\partial_\mu\partial_\nu$. The next term is

$$\begin{aligned} {R^{(2)}}_{\mu\nu} &= \partial_\rho {\Gamma^{(2)}}^\rho{}_{\mu\nu} - \partial_\nu {\Gamma^{(2)}}^\rho{}_{\mu\rho} + {\Gamma^{(1)}}^\rho{}_{\mu\nu}{\Gamma^{(1)}}^\sigma{}_{\rho\sigma} - {\Gamma^{(1)}}^\rho{}_{\mu\sigma}{\Gamma^{(1)}}^\sigma{}_{\rho\nu} \\ &= \frac{1}{2}\Big[\frac{1}{2}\partial_\mu h^{\rho\sigma}\partial_\nu h_{\rho\sigma} + h^{\sigma\rho}\left(\partial_\mu\partial_\nu h_{\rho\sigma} + \partial_\rho\partial_\sigma h_\mu\nu - \partial_\nu\partial_\rho h_{\mu\sigma} - \partial_\sigma\partial_\mu h_{\rho\nu}\right) \\ &\quad - \left(\partial_\sigma h^{\sigma\rho} - \frac{1}{2}\partial^\rho h\right)\left(\partial_\mu h_{\rho\mu} + \partial_\nu h_{\mu\rho} - \partial_\rho h_{\mu\nu}\right) + \partial^\rho h^\sigma_\nu\left(\partial_\rho h_{\sigma\mu} - \partial_\sigma h_{\rho\mu}\right)\Big] \\ &= \frac{1}{2}\Big\{\frac{1}{2}\partial_\mu\overline{h}_{\sigma\rho}\partial_\nu\overline{h}^{\sigma\rho} + \overline{h}^{\sigma\rho}\Big[\partial_\mu\partial_\nu\overline{h}_{\sigma\rho} + \partial_\sigma\partial_\rho\left(\overline{h}_{\mu\nu} - a_2 R^{(1)}\gamma_{\mu\nu}\right) \\ &\quad - \partial_\nu\partial_\rho\left(\overline{h}_{\sigma\mu} - a_2 R^{(1)}\gamma_{\sigma\mu}\right) - \partial_\mu\partial_\rho\left(\overline{h}_{\sigma\nu} - a_2 R^{(1)}\gamma_{\sigma\nu}\right)\Big] \\ &\quad + \partial^\rho\overline{h}^\sigma_\nu\left(\partial_\rho\overline{h}_{\sigma\mu} - \partial_\sigma\overline{h}_{\rho\mu}\right) - a_2\partial^\sigma R^{(1)}\partial_\sigma\overline{h}_{\mu\mu} + {a_2}^2\Big[2R^{(1)}\partial_\mu\partial_\nu R^{(1)} \\ &\quad + 3\partial_\mu R^{(1)}\partial_\nu R^{(1)} + R^{(1)}\Box^{(\mathrm{B})}R^{(1)}\gamma_{\mu\nu}\Big]\Big\}. \end{aligned} \tag{2.72}$$

To find the Ricci scalar we must contract the Ricci tensor, but we must decide which metric to use to do this. It is tempting to use the background metric, as we used this for raising the indices on $h_{\mu\nu}$, however this was just a notational convenience. The physical metric is the full metric, so we must use this to form R. Remembering that we are only considering terms to $\mathcal{O}(\epsilon^2)$, this gives

$$R^{(\mathrm{B})} = \gamma^{\mu\nu}{R^{(\mathrm{B})}}_{\mu\nu} \tag{2.73}$$

$$R^{(1)} = \gamma^{\mu\nu}{R^{(1)}}_{\mu\nu} \tag{2.74}$$

$$\begin{aligned} R^{(2)} &= \gamma^{\mu\nu}{R^{(2)}}_{\mu\nu} - h^{\mu\nu}{R^{(1)}}_{\mu\nu} \\ &= \gamma^{\mu\nu}{R^{(2)}}_{\mu\nu} - \overline{h}^{\mu\nu}{R^{(1)}}_{\mu\nu} + a_2{R^{(1)}}^2 \\ &= \frac{3}{4}\partial_\mu\overline{h}_{\sigma\rho}\partial^\mu\overline{h}^{\sigma\rho} - \frac{1}{2}\partial^\rho\overline{h}^{\sigma\mu}\partial_\sigma\overline{h}_{\rho\mu} - 2a_2\overline{h}^{\mu\nu}\partial_\mu\partial_\nu R^{(1)} \\ &\quad + a_2{R^{(1)}}^2 + \frac{3a_2}{2}\partial_\mu R^{(1)}\partial^\mu R^{(1)}. \end{aligned} \tag{2.75}$$

Using these

$$f^{(\mathrm{B})} = R^{(\mathrm{B})} \tag{2.76}$$

$$f^{(1)} = R^{(1)} \tag{2.77}$$

$$f^{(2)} = R^{(2)} + \frac{a_2}{2}{R^{(1)}}^2, \tag{2.78}$$

and

$$f'^{(\mathrm{B})} = a_2 R^{(\mathrm{B})} \tag{2.79}$$

$$f'^{(0)} = 1 \tag{2.80}$$

$$f'^{(1)} = a_2 R^{(1)} \tag{2.81}$$

$$f'^{(2)} = a_2 R^{(2)} + \frac{a_3}{2} {R^{(1)}}^2. \tag{2.82}$$

We list a zeroth order term here for clarity.

Using all of these

$$\begin{aligned}
{\mathcal{G}^{(2)}}_{\mu\nu} &= {R^{(2)}}_{\mu\nu} + f'^{(1)} {R^{(1)}}_{\mu\nu} - \partial_\mu\partial_\nu f'^{(2)} + {\Gamma^{(1)\rho}}_{\nu\mu}\partial_\rho f'^{(1)} + \gamma_{\mu\nu}\gamma^{\rho\sigma}\partial_\rho\partial_\sigma f'^{(2)} \\
&\quad - \gamma_{\mu\nu}\gamma^{\rho\sigma}{\Gamma^{(1)\lambda}}_{\sigma\rho}\partial_\lambda f'^{(1)} - \gamma_{\mu\nu}h^{\rho\sigma}\partial_\rho\partial_\sigma f'^{(1)} + h_{\mu\nu}\gamma^{\rho\sigma}\partial_\rho\partial_\sigma f'^{(1)} \\
&\quad - \frac{1}{2}f^{(2)}\gamma_{\mu\nu} - \frac{1}{2}f^{(1)}h_{\mu\nu} \\
&= {R^{(2)}}_{\mu\nu} + a_2 {R^{(1)}}{R^{(1)}}_{\mu\nu} - \partial_\mu\partial_\nu\left(a_2 R^{(2)} + \frac{a_3}{2}{R^{(1)}}^2\right) + {\Gamma^{(1)\rho}}_{\nu\mu}\partial_\rho\left(a_2 R^{(1)}\right) \\
&\quad + \gamma_{\mu\nu}\Box^{(\mathrm{B})}\left(a_2 R^{(2)} + \frac{a_3}{2}{R^{(1)}}^2\right) - \gamma_{\mu\nu}\gamma^{\rho\sigma}{\Gamma^{(1)\lambda}}_{\sigma\rho}\partial_\lambda\left(a_2 R^{(1)}\right) \\
&\quad - \gamma_{\mu\nu}h^{\rho\sigma}\partial_\rho\partial_\sigma\left(a_2 R^{(1)}\right) + h_{\mu\nu}\Box^{(\mathrm{B})}\left(a_2 R^{(1)}\right) - \frac{1}{2}\left(R^{(2)} + \frac{a_2}{2}{R^{(1)}}^2\right)\gamma_{\mu\nu} \\
&\quad - \frac{1}{2}R^{(1)}h_{\mu\nu} \\
&= {R^{(2)}}_{\mu\nu} + a_2\left(\gamma_{\mu\nu}\Box^{(\mathrm{B})} - \partial_\mu\partial_\nu\right)R^{(2)} - \frac{1}{2}R^{(2)}\gamma_{\mu\nu} + a_3\left(\gamma_{\mu\nu}\Box^{(\mathrm{B})} - \partial_\mu\partial_\nu\right){R^{(1)}}^2 \\
&\quad - \frac{1}{6}\overline{h}_{\mu\nu}R^{(1)} - a_2\gamma_{\mu\nu}\overline{h}^{\sigma\rho}\partial_\sigma\partial_\rho R^{(1)} + \frac{a_2}{2}\partial^\rho R^{(1)}\left(\partial_\mu\overline{h}_{\rho\nu} + \partial_\nu\overline{h}_{\rho\mu} - \partial_\rho\overline{h}_{\mu\nu}\right) \\
&\quad + a_2\left({R^{(1)}}{R^{(1)}}_{\mu\nu} + \frac{1}{4}{R^{(1)}}^2\gamma_{\mu\nu}\right) - {a_2}^2\left(\partial_\mu R^{(1)}\partial_\nu R^{(1)}\right. \\
&\quad \left. + \frac{1}{2}\gamma_{\mu\nu}\partial^\rho R^{(1)}\partial_\rho R^{(1)}\right)
\end{aligned} \tag{2.83}$$

It is simplest to split this up for the purposes of averaging. Since we average over all directions at each point gradients average to zero

$$\langle \partial_\mu V \rangle = 0. \tag{2.84}$$

As a corollary of this we have the relation

$$\langle U\partial_\mu V\rangle = -\langle \partial_\mu UV\rangle\,. \tag{2.85}$$

Repeated application of this, together with our gauge condition, equation (2.36), and wave equations, (2.27) and (2.42), allows us to eliminate many terms. Considering terms that do not trivially average to zero

$$\left\langle {R^{(2)}}_{\mu\nu}\right\rangle = \left\langle -\frac{1}{4}\partial_\mu\overline{h}_{\sigma\rho}\partial^\mu\overline{h}^{\rho\sigma} + \frac{{a_2}^2}{2}\partial_\mu R^{(1)}\partial_\nu R^{(1)} + \frac{a_2}{6}\gamma_{\mu\nu}R^{(1)}\right\rangle; \tag{2.86}$$

$$\left\langle R^{(2)} \right\rangle = \left\langle \frac{3a_2}{2} {R^{(1)}}^2 \right\rangle; \tag{2.87}$$

$$\left\langle \overline{h}_{\mu\nu} R^{(1)} \right\rangle = 0; \tag{2.88}$$

$$\left\langle R^{(1)} {R^{(1)}}_{\mu\nu} \right\rangle = \left\langle a_2 R^{(1)} \partial_\mu \partial_\nu R^{(1)} + \frac{1}{6} \gamma_{\mu\nu} {R^{(1)}}^2 \right\rangle. \tag{2.89}$$

Combining these gives

$$\left\langle {\mathcal{G}^{(2)}}_{\mu\nu} \right\rangle = \left\langle -\frac{1}{4} \partial_\mu \overline{h}_{\sigma\rho} \partial^\mu \overline{h}^{\rho\sigma} - \frac{3{a_2}^2}{2} \partial_\mu R^{(1)} \partial_\nu R^{(1)} \right\rangle. \tag{2.90}$$

Thus we obtain the result

$$t_{\mu\nu} = \frac{c^4}{32\pi G} \left\langle \partial_\mu \overline{h}_{\sigma\rho} \partial^\mu \overline{h}^{\rho\sigma} + 6{a_2}^2 \partial_\mu R^{(1)} \partial_\nu R^{(1)} \right\rangle. \tag{2.91}$$

In the limit of $a_2 \to 0$ we obtain the standard GR result as required. Note that the GR result is also recovered if $R^{(1)} = 0$, as would be the case if the Ricci mode was not excited, for example if the frequency was below the cut off frequency m. Rewriting the pseudotensor in terms of metric perturbation $h_{\mu\nu}$, using equation (2.57), we obtain

$$t_{\mu\nu} = \frac{c^4}{32\pi G} \left\langle \partial_\mu h_{\sigma\rho} \partial^\mu h^{\rho\sigma} + \frac{1}{8} \partial_\mu h \partial_\nu h \right\rangle. \tag{2.92}$$

2.5 Radiation With A Source

Having consider radiation in a vacuum, we now move on to consider the case with a source term. We want a first order perturbation from our background metric so that the linearised field equation is

$${\mathcal{G}^{(1)}}_{\mu\nu} = \frac{8\pi G}{c^4} T_{\mu\nu}. \tag{2.93}$$

Again assuming a Minkowski background, our first order field equations are

$${\mathcal{G}^{(1)}}_{\mu\nu} = {R^{(1)}}_{\mu\nu} - \partial_\mu \partial_\nu (a_2 R^{(1)}) + \eta_{\mu\nu} \Box (a_2 R^{(1)}) - \frac{R^{(1)}}{2} \eta_{\mu\nu} \tag{2.94}$$

$$\mathcal{G}^{(1)} = 3a_2 \Box R^{(1)} - R^{(1)} \tag{2.95}$$

where $\mathcal{G}^{(1)} = \eta^{\mu\nu} {\mathcal{G}^{(1)}}_{\mu\nu}$. Will we again use our ansatz $\overline{h}_{\mu\nu}$ from equation (2.33), with $b = -1$. The Ricci tensor is

$${R^{(1)}}_{\mu\nu} = \frac{1}{2} \left[2a_2 \partial_\mu \partial_\nu R^{(1)} - \Box \left(\overline{h}_{\mu\nu} - \frac{\overline{h}}{2} \eta_{\mu\nu} \right) + \frac{a_2}{2} \Box R^{(1)} \eta_{\mu\nu} \right]. \tag{2.96}$$

Taking the traces gives

$$R^{(1)} = 3a_2 \Box R^{(1)} + \frac{1}{2} \Box \overline{h} \tag{2.97}$$

just as in equation (2.40). Comparing this with the trace of the field equation yields

$$-\frac{1}{2}\Box\overline{h} = \mathcal{G}^{(1)} \tag{2.98}$$

Using this with our expression for the Ricci tensor in the field equation gives

$$\begin{aligned}\mathcal{G}^{(1)}{}_{\mu\nu} &= a_2\partial_\mu\partial_\nu R^{(1)} - \frac{1}{2}\Box\overline{h}_{\mu\nu} + \frac{1}{2}\Box\left(\frac{\overline{h}}{2} + a_2 R^{(1)}\right)\eta_{\mu\nu} - a_2\partial_\mu\partial_\nu R^{(1)} \\ &\quad + a_2\Box R^{(1)}\eta_{\mu\nu} - \frac{1}{2}R^{(1)}\eta_{\mu\nu} \\ &= -\frac{1}{2}\Box\overline{h}_{\mu\nu}.\end{aligned} \tag{2.99}$$

We see that our field equations are consistent.

2.6 Discussion & Remaining Questions

Chapter 3

Parabolic Encounters Of A Massive Black Hole

3.1 Background & Introduction

Currently it is understood that many, if not all at some point, galactic nuclei harbour a black hole[9, 10]. The best opportunity to study these objects comes from the compact object in our own galactic centre, which is coincident with Sagittarius A*. This is identified as a massive black hole (MBH) of mass $M_\bullet = 4M_\odot$ and a distance of only $R_0 = 8\,\mathrm{kpc}$. According to the no-hair theorem the MBH should be described completely by its mass $M_\bullet$ and spin a (since we do not expect an astrophysical black hole to be charged)[11–16]. Consequently, measuring the spin is necessary to fully understand the MBH and its rôle in the evolution of the Galaxy. It has been suggested that the spin could be inferred from careful observation of the orbits of stars within a few millparsecs of the Galactic centre[17], although this is complicated because of perturbations due to other stars, or from observations of quasi-periodic oscillations (QPOs) of radio emissions[18]: this latter method has produced a value of for dimensionless spin, $a_* = Jc/GM_\bullet^2$ where J is the MBH's angular momentum, of $a_* = 0.44 \pm 0.08$, though this also uses observations of Galactic X-ray sources, containing solar mass BHs, to find a best-fit unique spin parameter for all BHs.

An exciting means of inferring information about the Galactic MBH is through gravitational waves (GWs) emitted when compact objects (COs), such as smaller BHs, neutron stars (NSs), white dwarfs (WDs) or low mass main sequence (MS) stars, pass close by. The planned NASA/ESA Laser Interferometer Space Antenna (LISA) is designed to be able to detect GWs in the frequency range of interest for these encounters[19, 20]. The identification of waves requires a set of accurate waveform templates covering parameter space. Much work has already been done on the waveforms generated when companion objects inspiral towards an MBH; as they orbit, the GWs carry away energy and angular momentum, causing the orbit to shrink until eventually the object plunges into the MBH. The initial orbits may be highly elliptical and a burst of radiation is emitted during each close encounter. These are known as extreme mass ratio bursts (EMRBs)[21]. Assuming that the companion is not scattered from its orbit,

and does not plunge straight into the MBH, its orbit will evolve, becoming more circular, and it will begin to emit continuously significant gravitational radiation. The resulting waveforms are known as extreme mass ratio inspirals (EMRIs).

Studies of these systems have usually focused upon when the orbit completes multiple cycles, thus allowing a high signal-to-noise ratio to be accumulated. Here, we will investigate what can be learnt from high eccentricity orbits. These are the initial orbits onto which we expect that COs may be scattered by interactions with other bodies. We will make the simplifying assumption that all these orbits are marginally bound, or parabolic, since highly eccentric orbits will appear almost indistinguishable from an appropriate parabolic orbit [22]. Here "parabolic" and "eccentricity" refer to the energy of the geodesic and not to the geometric shape of the orbit.[1] Following such a trajectory an object may make just one pass of the MBH or, if the periapsis distance is small enough, it may complete a number or rotations. Such an orbit is referred to as zoom-whirl.

In order to compute the gravitational waveform produced in such as case, we integrate the geodesic equations for a parabolic orbit in Kerr spacetime. We assume that the orbiting body is a test particle, such that it does not influence the underlying spacetime, and that the orbital parameters evolve negligibly during the orbit so that they may be held constant. We use this to construct an approximate numerical kludge waveform [23].

3.2 Parabolic Orbits in Kerr Spacetime

3.2.1 The Metric & Geodesic Equations

Astrophysical BHs are described by the Kerr metric [24]. In standard Boyer-Lindquist coordinates the line element is [25, 26]

$$\mathrm{d}s^2 = \frac{\rho^2 \Delta}{\Sigma^2} c^2 \mathrm{d}t^2 - \frac{\Sigma \sin^2\theta}{\rho^2} \left(\mathrm{d}\phi - \omega \mathrm{d}t\right)^2 - \frac{\rho^2}{\Delta} \mathrm{d}r^2 - \rho^2 \mathrm{d}\theta^2, \tag{3.1}$$

where we have introduced functions

$$\rho^2 = r^2 + a^2 \cos^2\theta, \tag{3.2}$$

$$\Delta = r^2 - \frac{2GM_\bullet r}{c^2} + a^2, \tag{3.3}$$

$$\Sigma = \left(r^2 + a^2\right)^2 - a^2 \Delta \sin^2\theta, \tag{3.4}$$

$$\omega = \frac{2GM_\bullet a r}{c\Sigma}. \tag{3.5}$$

The spin parameter is related to the BH's angular momentum by

$$J = M_\bullet a c. \tag{3.6}$$

For the remainder of this section we shall work in natural units with $G = c = 1$.

Geodesics are parameterized by three conserved quantities (aside from the particle's mass μ): the energy (per unit mass) E, the specific angular momentum about the

[1] Marginally bound Keplerian orbits in flat spacetime are parabolic in both senses.

symmetry axis (the z-axis) L_z, and Carter's constant Q[16, 27]. The geodesic equations are

$$\rho^2 \frac{\mathrm{d}t}{\mathrm{d}\tau} = a\left(L_z - aEz\sin^2\theta\right) + \frac{r^2+a^2}{\Delta}T, \tag{3.7}$$

$$\rho^2 \frac{\mathrm{d}r}{\mathrm{d}\tau} = \pm\sqrt{V_r}, \tag{3.8}$$

$$\rho^2 \frac{\mathrm{d}\theta}{\mathrm{d}\tau} = \pm\sqrt{V_\theta}, \tag{3.9}$$

$$\rho^2 \frac{\mathrm{d}\phi}{\mathrm{d}\tau} = \frac{L_z}{\sin^2\theta} - aE + \frac{a}{\Delta}T, \tag{3.10}$$

$$\tag{3.11}$$

where we have introduced potentials

$$T = E\left(r^2+a^2\right) - aL_z, \tag{3.12}$$

$$V_r = T^2 - \Delta\left[r^2 + (L_z - aE)^2 + Q\right], \tag{3.13}$$

$$V_\theta = Q - \cos^2\theta\left[a^2\left(1-E^2\right) + \frac{L_z^2}{\sin^2\theta}\right], \tag{3.14}$$

and τ is proper time. The signs of the r and θ equations may be chosen independently.

For a parabolic orbit $E = 1$, thus the particle is at rest at infinity. This simplifies the geodesic equations. It also allows us to give a simple interpretation for Carter's constant Q: this is defined such that

$$Q = L_\theta^2 + \cos^2\theta\left[a^2\left(1-E^2\right) + \frac{L_z^2}{\sin^2\theta}\right], \tag{3.15}$$

where L_θ is the (non-conserved) specific angular momentum in the θ direction (note $L_\theta^2 = V_\theta$). For $E = 1$ we have

$$\begin{aligned} Q &= L_\theta^2 + \cot^2\theta\, L_z^2 \\ &= L_\infty^2 - L_z^2 \end{aligned} \tag{3.16}$$

where L_∞ is the total specific angular momentum at infinity, where the metric is asymptotically flat[28].[2] This is just as in the Schwarzschild case.

3.2.2 Integration Variables & Turning Points

In integrating the geodesic equations difficulties can arise because of the presence of turning points in the motion, when the sign of the r or θ geodesic equation will change sign. The radial turning points are at the periapsis r_p and at infinity. We may find the location of the periapsis by finding the roots of

$$V_r = 0$$

$$2M_\bullet r^3 - \left(L_z^2 + Q\right)r^2 + 2M_\bullet\left[(L_z - a)^2 + Q\right]r - a^2 Q = 0. \tag{3.17}$$

[2] See Rosquist, Bylund & Samuelsson[29] for an interesting discussion of the interpretation of Q in the limit $G \to 0$ corresponding to a flat spacetime.

This has three roots, which we shall denote $\{r_1, r_2, r_p\}$; the periapsis r_p is the largest real root. We do not find the apoapsis as a (fourth) root to this equation as we have removed it by taking $E = 1$ before solving: it is simple to show this is a turning point by setting the unconstrained expression for V_r equal to zero, and then solving for $E(r)$; taking the limit $r \to \infty$ gives $E \to 1$, so parabolic orbits do have a stationary point at infinity [30]. We may avoid the difficulties of the turning point by introducing an angular variable that always increases with proper time [31]: inspired by Keplerian orbits, we may parameterize our parabolic trajectory by

$$r = \frac{p}{1 - e\cos\psi}, \tag{3.18}$$

where $e = 1$ is the eccentricity and $p = 2r_p$ is the semilatus rectum. As ψ covers its full range from 0 to 2π, r traces out one full orbit from infinity through the periapsis at $\psi = \pi$ back to infinity. The geodesic equation for ψ is

$$\rho^2 \frac{\mathrm{d}\psi}{\mathrm{d}\tau} = \left\{ M_\bullet \left[2r_p - (r_1 + r_2)(1 + \cos\psi) + \frac{r_1 r_2}{2r_p}(1 + \cos\psi)^2 \right] \right\}^{1/2}. \tag{3.19}$$

This may be integrated without problem. Parameterizing an orbit by its periapsis and eccentricity has the additional benefit of allowing easier comparison with its flat-space equivalent than considering energy and angular momentum [32].

The θ motion is (usually) bounded, with $\theta_0 \leq \theta \leq \pi - \theta_0$. The turning points are given by where

$$\begin{aligned} V_\theta &= 0 \\ Q - \cot^2\theta\, L_z^2 &= 0. \end{aligned} \tag{3.20}$$

Note that only if $L_z = 0$ may we reach the poles [30]. If we change variable to $\zeta = \cos^2\theta$, we have a maximum value $\zeta_0 = \cos^2\theta_0$ given by

$$\zeta_0 = \frac{Q}{Q + L_z^2} \tag{3.21}$$

$$= \frac{Q}{L_\infty^2}. \tag{3.22}$$

See figure 3.1 for a geometrical visualization. Let us now introduce a second angular

Figure 3.1: The angular momenta L_∞, L_z and $\sqrt{Q}$ define a right-angled triangle. The acute angles are θ_0, the extremal value of the polar angle, and ι, the orbital inclination [33].

variable [31]

$$\zeta = \zeta_0 \cos^2\chi. \tag{3.23}$$

Over one 2π period of χ, θ oscillates over its full range, from its minimum value to its maximum and back. The geodesic equation for χ is

$$\rho^2 \frac{\mathrm{d}\chi}{\mathrm{d}\tau} = \sqrt{Q + L_z^2}, \tag{3.24}$$

and may be integrated simply.

3.3 Waveform Construction

With the geodesic calculated for given angular momenta L_z and Q, and initial starting positions, the orbiting body is assumed to follow this trajectory exactly: we ignore evolution due to the radiation of energy and angular momentum. From this we calculate the gravitational waveform using a semirelativistic approximation[34]: we assume that the particle moves along a geodesic in the Kerr geometry, but radiates as if it were in flat spacetime. This quick-and-dirty technique is known as a numerical kludge[23].

3.3.1 Kludge Approximation

Numerical kludge approximations aim to encapsulate the main characteristics of a waveform by using the exact particle trajectory (ignoring inaccuracies from the evolution of the orbital parameters), whilst saving on computational time by using approximate waveform generation techniques. To start, we build an equivalent flat spacetime trajectory from the Kerr geodesic. This is done by identifying the Boyer-Lindquist coordinates with a set of flat-space coordinates; we consider two choices here:

1. Identify the Boyer-Lindquist coordinates with flat-space spherical polars $\{r_{\mathrm{BL}}, \theta_{\mathrm{BL}}, \phi_{\mathrm{BL}}\} \rightarrow \{r_{\mathrm{sph}}, \theta_{\mathrm{sph}}, \phi_{\mathrm{sph}}\}$, then define flat-space Cartesian coordinates[23, 32]

$$\boldsymbol{x} = (r_{\mathrm{sph}} \sin\theta_{\mathrm{sph}} \cos\phi_{\mathrm{sph}}, r_{\mathrm{sph}} \sin\theta_{\mathrm{sph}} \sin\phi_{\mathrm{sph}}, r_{\mathrm{sph}} \cos\theta_{\mathrm{sph}}) \,. \tag{3.25}$$

2. Identify the Boyer-Lindquist coordinates with flat-space oblate-spheroidal coordinates $\{r_{\mathrm{BL}}, \theta_{\mathrm{BL}}, \phi_{\mathrm{BL}}\} \rightarrow \{r_{\mathrm{ob}}, \theta_{\mathrm{ob}}, \phi_{\mathrm{ob}}\}$ so that the flat-space Cartesian coordinates are

$$\boldsymbol{x} = \left(\sqrt{{r_{\mathrm{ob}}}^2 + a^2} \sin\theta_{\mathrm{ob}} \cos\phi_{\mathrm{ob}}, \sqrt{{r_{\mathrm{ob}}}^2 + a^2} \sin\theta_{\mathrm{ob}} \sin\phi_{\mathrm{ob}}, r_{\mathrm{ob}} \cos\theta_{\mathrm{ob}}\right) . \tag{3.26}$$

   These are appealing since in the limit of $G \rightarrow 0$, so that the gravitating mass goes to zero, the Kerr metric in Boyer-Lindquist coordinates reduces to the Minkowski metric in oblate spheroidal coordinates.[3]

In the limit of $a \rightarrow 0$, the two coincide, as they do in the limit of large r_{BL}. It must be stressed that there is no well motivated argument that either coordinate system must yield an accurate GW; their use is justified *post facto* by comparison with result obtained from more accurate, and computationally intensive, methods[23, 32]. This ambiguity in assigning flat-space coordinates reflects the inconsistency of the semi-relativistic approximation: the geodesic trajectory was calculated for the Kerr geometry; by moving to flat spacetime we lose the reason for its existence. However, this inconsistency should not be regarded as a major problem; it is just an artifact of the basic assumption that the shape of the trajectory is important for determining the character of the radiation, but the curvature of the spacetime in the vicinity of the source is not. By binding the particle

[3] We must take the limit $G \rightarrow 0$, rather than $M_\bullet \rightarrow 0$ to avoid the problem of an over-extreme BH with $a > M_\bullet$.

to the exact geodesic, we ensure that the kludge waveform has spectral components at the correct frequencies, but by assuming flat spacetime for generation of GWs they will not have the correct amplitudes.

3.3.2 Quadrupole-Octopole Formula

Now we have a flat-space particle trajectory ${x_\mathrm{p}}^\mu(\tau)$, we may apply a flat-space wave generation formula. We shall use the quadrupole-octopole formula to calculate the gravitational strain[35, 36]

$$h^{jk}(t,\boldsymbol{x}) = -\frac{2G}{c^6 r}\left[\ddot{I}^{jk} - 2n_i\ddot{S}^{ijk} + n_i\dddot{M}^{ijk}\right]_{t'=t-cr} \tag{3.27}$$

where an overdot represents differentiation with respect to time t, t' is the retarded time, $r = |\boldsymbol{x} - \boldsymbol{x}_\mathrm{p}|$ is the radial distance, $\boldsymbol{n}$ is the radial unit vector, and the mass quadrupole I^{jk}, current quadrupole S^{ijk} and mass octopole M^{ijk} are defined by

$$I^{jk}(t') = \int x'^j x'^k T^{00}(t', \boldsymbol{x'})\,\mathrm{d}^3x' \tag{3.28}$$

$$S^{ijk}(t') = \int x'^j x'^k T^{0i}(t', \boldsymbol{x'})\,\mathrm{d}^3x' \tag{3.29}$$

$$M^{ijk}(t') = \frac{1}{c}\int x'^i x'^j x'^k T^{00}(t', \boldsymbol{x'})\,\mathrm{d}^3x'. \tag{3.30}$$

This is correct for a slow moving source. It is the familiar quadrupole formula[5, 26], derived from linearized theory, but with the next order term included. For a point mass the energy-momentum tensor $T^{\mu\nu}$ contains a δ-function which allows easy evaluation of the integrals of the various moments to give

$$I^{jk} = c^2\mu x_\mathrm{p}^j x_\mathrm{p}^k \tag{3.31}$$

$$S^{ijk} = c\mu v_\mathrm{p}^i x_\mathrm{p}^j x_\mathrm{p}^k \tag{3.32}$$

$$M^{ijk} = c\mu x_\mathrm{p}^i x_\mathrm{p}^j x_\mathrm{p}^k. \tag{3.33}$$

To evaluate equation (3.27) we need up to the third time derivative of the position. The velocity $\boldsymbol{v}_\mathrm{p} = \dot{\boldsymbol{x}}_\mathrm{p}$ can be calculated from the geodesic equations: dividing by $\mathrm{d}t/\mathrm{d}\tau$ gives $\dot{r}$, $\dot{\theta}$ and $\dot{\phi}$ which can then be transformed to the Cartesian velocities assuming either the spherical or oblate spheroidal coordinate system.[4] Expressions for the acceleration $\boldsymbol{a}_\mathrm{p} = \ddot{\boldsymbol{x}}_\mathrm{p}$ and the jerk $\boldsymbol{j}_\mathrm{p} = \dddot{\boldsymbol{x}}_\mathrm{p}$ are more involved, so these derivatives are found numerically using a simple difference formula to approximate the derivative as

$$\left.\frac{\mathrm{d}f}{\mathrm{d}t}\right|_{t_1} \approx \frac{1}{2}\left[\frac{f(t_1) - f(t_0)}{t_1 - t_0} + \frac{f(t_2) - f(t_1)}{t_2 - t_1}\right], \tag{3.34}$$

where t_0, t_1 and t_2 are subsequent (not necessarily uniformly spaced) time-steps.

[4] There is again the problem of the sign of the geodesic equations, this is simply solved by taking the sign as calculated by finite differencing the trajectory.

Since we are only interested in GWs, we shall use the transverse-traceless (TT) gauge. The waveform is given in the TT gauge by[5]

$$h^{\mathrm{TT}}{}_{jk} = P^l_j h_{lm} P^m_k - \frac{1}{2} P_{jk} P^{lm} h_{lm}, \tag{3.35}$$

where the (spatial) projection operator P_{ij} is

$$P_{ij} = \delta_{ij} - n_i n_j. \tag{3.36}$$

3.4 Detection With LISA

The LISA detector is a three-arm, space-Borneo laser interferometer[19, 20]. The three arms form an equilateral triangle that rotates as the system's centre of mass follows a circular, heliocentric orbit, trailing 20° behind the Earth. To describe the detector configuration, and to transform from the MBH coordinate system to those of the detector, we will find it useful to define three coordinate systems: those of the BH at the galactic centre $x^i_\bullet$; ecliptic coordinates centred at the solar system barycentre $x^i_\odot$, and coordinates that co-rotate with the detector x^i_{d}. The currently envisioned mission geometry is depicted in figures (??). The coordinate systems are related by a series of angles: Θ and Φ give the orientation of the solar system in the MBH's coordinates, these define the orientation of the MBH's spin axis $z_\bullet$; $\overline{\Theta}$ and $\overline{\Phi}$ give the position of the galactic centre in ecliptic coordinates; $\overline{\phi}$ gives LISA's orbital phase and φ gives the rotational phase of the detector arms, both of these vary linearly with time

$$\overline{\phi}(t) = \omega_\oplus t + \overline{\phi}_0; \quad \varphi(t) = -\omega_\oplus t + \varphi_0; \tag{3.37}$$

where $\omega_\oplus$ corresponds to one rotation per year; finally, $\alpha = 60°$ is the inclination of the detector plane. We have computed the waveforms in the MBH's coordinates, however it is simplest to describe the measured signal using the detector's coordinates. To transform between coordinates we will use the matrix A_{ij}:

$$x^i_{\mathrm{d}} = A_{ij} x^j_\bullet; \quad h^{ij}_{\mathrm{d}} = A_{ik} A_{jl} h^{kl}_\bullet. \tag{3.38}$$

To define this, it is convenient to introduce angles

$$\Sigma = \overline{\Theta} + \Theta; \quad \delta = \overline{\phi} - \overline{\Phi}. \tag{3.39}$$

The transformation matrix from the BH coordinates to the detector coordinates is

$$[A_{ij}] = \begin{pmatrix} a_{11} & a_{12} & a_{13} \\ a_{21} & a_{22} & a_{23} \\ a_{31} & a_{32} & a_{33} \end{pmatrix}; \tag{3.40}$$

the elements are

$$a_{11} = s_\varphi \left(c_\delta s_\Phi - s_\delta c_\Phi c_\Sigma\right) - c_\varphi \left[s_\alpha c_\Phi s_\Sigma - c_\alpha \left(c_\delta c_\Phi c_\Sigma + s_\delta s_\Sigma\right)\right]; \tag{3.41}$$

$$a_{12} = -s_\varphi \left(c_\delta c_\Phi - s_\delta s_\Phi c_\Sigma\right) - c_\varphi \left[s_\alpha s_\Phi s_\Sigma - c_\alpha \left(c_\delta s_\Phi c_\Sigma + s_\delta s_\Sigma\right)\right]; \tag{3.42}$$

$$a_{13} = s_\varphi s_\delta s_\Sigma - c_\varphi \left(s_\alpha c_\Sigma + c_\alpha c_\delta s_\Sigma\right); \tag{3.43}$$

$$a_{21} = s_\varphi \left[s_\alpha c_\Phi s_\Sigma - c_\alpha \left(c_\delta c_\Phi c_\Sigma + s_\delta s_\Sigma\right)\right] - c_\varphi \left(c_\delta s_\Phi - s_\delta c_\Phi s_\Sigma\right); \tag{3.44}$$

$$a_{22} = s_\varphi \left[s_\alpha s_\Phi s_\Sigma - c_\alpha \left(c_\delta s_\Phi c_\Sigma + s_\delta s_\Sigma\right)\right] - c_\varphi \left(c_\delta c_\Phi - s_\delta s_\Phi s_\Sigma\right); \tag{3.45}$$

$$a_{23} = s_\varphi \left(s_\alpha c_\Sigma + c_\alpha c_\delta s_\Sigma\right) - c_\varphi s_\delta s_\Sigma; \tag{3.46}$$

$$a_{31} = -s_\alpha \left(c_\delta c_\Phi c_\Sigma + s_\delta s_\Phi\right) - c_\alpha c_\Phi s_\Sigma; \tag{3.47}$$

$$a_{32} = s_\alpha \left(s_\delta c_\Phi - c_\delta s_\Phi c_\Sigma\right) - c_\alpha s_\Phi s_\Sigma; \tag{3.48}$$

$$a_{33} = s_\alpha c_\delta s_\Sigma - c_\alpha c_\Sigma; \tag{3.49}$$

where we define $s_\vartheta \equiv \sin\vartheta$ and $c_\vartheta \equiv \cos\vartheta$.

The strains measured in the three arms can be combined such that LISA behaves as a pair of 90° interferometers at 45° to each other (with signals scaled by $\sqrt{3}/2$)[37]. We will denote the two detectors as I and II. If we label the change in the three arms lengths caused by GWs δL_1, δL_2 and δL_3, and use L for the unstrained length, then detector I measures strain

$$h_{\rm I}(t) = \frac{\delta L_1 - \delta L_2}{L} \tag{3.50}$$

$$= \frac{\sqrt{3}}{2}\left(\frac{1}{2}h_{\rm d}^{xx} - \frac{1}{2}h_{\rm d}^{yy}\right), \tag{3.51}$$

and detector II measures

$$h_{\rm II}(t) = \frac{\delta L_1 + \delta L_2 - 2\delta L_3}{\sqrt{3}L} \tag{3.52}$$

$$= \frac{\sqrt{3}}{2}\left(\frac{1}{2}h_{\rm d}^{xy} + \frac{1}{2}h_{\rm d}^{yx}\right). \tag{3.53}$$

We will use vector notation $\boldsymbol{h}(t) = (h_{\rm I}(t), h_{\rm II}(t)) = \{h_A(t)\}$ to represent signals from both detectors.

The final consideration for calculating the signal measured by LISA is the time of arrival of the signal: LISA's orbital position changes with time. Fortunately over the timescales of interest for parabolic encounters, these changes are small. We will assume that the position of the solar system barycentre relative to the galactic centre is constant, at least over these short timescales: it is defined by the distance R_0 and the angles $\overline{\Theta}$ and $\overline{\Phi}$. The time of arrival at the solar system barycentre $t_\odot$ is then the appropriate retarded time. The time of detection $t_{\rm d}$ to lowest order is then

$$t_{\rm d} \simeq t_\odot - t_{\rm AU}\cos\left[\overline{\phi}(t_\odot) - \overline{\Phi}\right]\sin\overline{\Theta}, \tag{3.54}$$

where $t_{\rm AU}$ is the light travel-time for LISA's orbital radius. The time $t_{\rm d}$ must be used for $\phi(t)$ and $\varphi(t)$.

3.5 Signal Analysis

3.5.1 Frequency Domain Formalism

At this stage we now know the GW $\boldsymbol{h}(t)$ that will be incident upon the LISA detector. We must now discuss how to analyse the waveform to extract the information it contains. We begin with a brief overview of the basic components of signal analysis used for GWs, with application to LISA in particular. This fixes the notation we will employ. A more complete discussion of material presented here can be found in the work of Finn[38], and Cutler and Flanagan[39].

The actual measured strain $\boldsymbol{s}(t)$ will be the combination of the signal and the detector noise

$$\boldsymbol{s}(t) = \boldsymbol{h}(t) + \boldsymbol{n}(t), \tag{3.55}$$

we will assume that the noise $n_A(t)$ is stationary and Gaussian. When analysing signals, it is most convenient to work with the Fourier transform

$$\tilde{g}(f) = \int_{-\infty}^{\infty} g(t) e^{2\pi i f t} \, \mathrm{d}t. \tag{3.56}$$

Since we have assumed Gaussianity for the noise signal $n_A(t)$, each Fourier component $\tilde{n}_A(f)$ also has a Gaussian probability distribution; the assumption of stationarity means that different Fourier components are uncorrelated, thus[39]

$$\left\langle \tilde{n}_A(f) \tilde{n}_B^*(f') \right\rangle_n = \frac{1}{2} \delta(f - f') S_{AB}(f), \tag{3.57}$$

where $\langle \ldots \rangle_n$ denotes the expectation value over the noise distribution, and $S_{AB}(f)$ is the (single-sided) noise spectral density. For simplicity, we may assume that the noise in the two detectors are uncorrelated, but share the same characterization so that[37]

$$S_{AB}(f) = \delta_{AB} S_n(f). \tag{3.58}$$

The functional form of the noise spectral density $S_n(f)$ for LISA is discussed below in section 3.5.2.

The properties of the noise allow us to define a natural inner product and associated distance on the space of signals[39]

$$(\boldsymbol{g}|\boldsymbol{k}) = 2 \int_0^{\infty} \frac{\tilde{g}_A^*(f) \tilde{k}_A(f) + \tilde{g}_A(f) \tilde{k}_A^*(f)}{S_n(f)} \, \mathrm{d}f. \tag{3.59}$$

Using this definition, the probability of a particular realization of noise $\boldsymbol{n}(t) = \boldsymbol{n}_0(t)$ is

$$p(\boldsymbol{n}(t) = \boldsymbol{n}_0(t)) \propto \exp\left[-\frac{1}{2} (\boldsymbol{n}_0 | \boldsymbol{n}_0) \right]. \tag{3.60}$$

Thus, if the incident waveform is given as $\boldsymbol{h}(t)$, the probability of measuring signal $\boldsymbol{s}(t)$ is

$$p(\boldsymbol{s}(t) | \boldsymbol{h}(t)) \propto \exp\left[-\frac{1}{2} (\boldsymbol{s} - \boldsymbol{h} | \boldsymbol{s} - \boldsymbol{h}) \right]. \tag{3.61}$$

3.5.2 LISA Noise Curve

LISA's noise has two sources: instrumental noise and confusion noise, primarily from white dwarf binaries. The latter may be divided into contributions from galactic and extragalactic binaries. In this work we use the noise model of Barack and Cutler [40]. The shape of the noise curve can be seen figures (??). The instrumentation noise dominates at both high and low frequencies. The confusion noise is important at intermediate frequencies, and is responsible for the cusp around $f = 1 \times 10^{-3}\,\mathrm{Hz}$.

3.5.3 Window Functions

There is one remaining complication regarding signal analysis. When we perform a Fourier transform using a computer we must necessarily only transform a finite time-span (it is a discrete Fourier transform).[5] The effect of which is the same as transforming the true, infinite signal multiplied by a unit top hat function of width equal to the time-span. Fourier transforming this yields the true waveform convolved with a sinc. If $\tilde{h}'(f)$ is the computed Fourier transform then

$$\tilde{h}'(f) = \int_0^\tau h(t) e^{2\pi i f t}\,\mathrm{d}t \tag{3.62}$$

$$= \left[\tilde{h}(f) * e^{-\pi i f \tau}\tau \mathrm{sinc}(\pi f \tau)\right], \tag{3.63}$$

where $\tilde{h}(f) = \mathscr{F}\{h(t)\}$, is the unwindowed Fourier transform. This windowing of the data is an inherent problem in the method; it will be as much of a problem when analysing signals from LISA as it is computing waveforms here. Windowing causes spectral leakage, which means that a contribution from large amplitude spectral components leaks into other components (side lobes), obscuring and distorting the spectrum at these frequencies [41].

Figure (??) shows the computed Fourier transforms for an example parabolic encounter. The waveforms have two distinct regions: a low-frequency curve, and a high-frequency tail. The low-frequency signal is the spectrum we are interested in; the high-frequency components are the result of spectral leakage. The $\mathcal{O}(1/f)$ behaviour of the sinc gives the shape of the tail. This has possibly been misidentified by Burko and Khanna [42] as the characteristic strain for parabolic encounters.

Despite being many orders of magnitude below the peak level, the high-frequency tail is still well above the noise curve for a wide range of frequencies. It will therefore contribute to the evaluation of any inner products, and may mask interesting features. Unfortunately this is a fundamental problem that cannot be resolved completely. However, it is possible to the reduce the amount of spectral leakage using apodization: to improve the frequency response of a finite time series one can use a number of weighting window functions $w(t)$ which modify the impulse response in a prescribed way. The simplest window function is the rectangular (or Dirichlet) window; this is just the top hat described above. Other window functions are generally tapered. The introduction of a window function influences the spectrum in a manner dependent upon its precise shape;

[5] The time-span in this case is the length of time the trajectory was calculated for.

there are two distinct distortions: local smearing due to the finite width of the centre lobe, and distant leakage due to finite amplitude side lobes. Choosing a window-function is a trade-off between these two sources of error.

3.6 Parameter Estimation

Having detected a GW signal $\boldsymbol{s}(t)$ we are interested in what we may infer about the source. Let us define $\boldsymbol{\lambda} = \{\lambda^1, \lambda^2, \ldots, \lambda^N\}$ as the set of N parameters which define the GW. We have a inference problem that may be solved by appropriate application of Bayes' Theorem[43]: the probability distribution for our parameters given that we have detected the signal $\boldsymbol{s}(t)$ is given by the posterior

$$p(\boldsymbol{\lambda}|\boldsymbol{s}(t)) = \frac{p(\boldsymbol{s}(t)|\boldsymbol{\lambda})p(\boldsymbol{\lambda})}{p(\boldsymbol{s}(t))}. \tag{3.64}$$

Here $p(\boldsymbol{s}(t)|\boldsymbol{\lambda})$ is the likelihood of the parameters, $p(\boldsymbol{\lambda})$ is the prior probability distribution for the parameters, and $p(\boldsymbol{s}(t)) = \int p(\boldsymbol{s}(t)|\boldsymbol{\lambda})\,\mathrm{d}^N\lambda$ is, for our purposes a normalising constant, and may be ignored. The likelihood function depends upon the particular realization of noise. A particular set of parameters $\boldsymbol{\lambda}_0$ defines a waveform $\boldsymbol{h}_0(t) = \boldsymbol{h}(t;\boldsymbol{\lambda}_0)$, the probability that we observe signal $\boldsymbol{s}(t)$ for this GW is given by equation (3.61), so the likelihood is just

$$p(\boldsymbol{s}(t)|\boldsymbol{\lambda}_0) \propto \exp\left[-\frac{1}{2}\left(\boldsymbol{s}-\boldsymbol{h}_0|\boldsymbol{s}-\boldsymbol{h}_0\right)\right]. \tag{3.65}$$

If we were to define this as a probability distribution for the parameters $\boldsymbol{\lambda}$, then the modal values would be the maximum-likelihood parameters $\boldsymbol{\lambda}_{\mathrm{ML}}$. The waveform $h(t;\boldsymbol{\lambda}_{\mathrm{ML}})$ would be the signal closest to $\boldsymbol{s}(t)$ in the space of all signal, where distance is defined using the inner product[39].

In the limit of a high signal-to-noise ratio (SNR), we may approximate this as[44]

$$p(\boldsymbol{s}(t)|\boldsymbol{\lambda}_0) \propto \exp\left[-\frac{1}{2}\left(\partial_a\boldsymbol{h}|\partial_b\boldsymbol{h}\right)\left(\lambda^a - \langle\lambda^a\rangle_\ell\right)\left(\lambda^b - \langle\lambda^b\rangle_\ell\right)\right], \tag{3.66}$$

where the mean is defined as

$$\langle\lambda^a\rangle_\ell = \frac{\int \lambda^a p(\boldsymbol{s}(t)|\boldsymbol{\lambda})\,\mathrm{d}^N\lambda}{\int p(\boldsymbol{s}(t)|\boldsymbol{\lambda})\,\mathrm{d}^N\lambda}. \tag{3.67}$$

Using the high SNR limit approximation, this mean is just the maximum-likelihood value $\langle\lambda^a\rangle_\ell = \lambda^a_{\mathrm{ML}}$. The quantity

$$\Gamma_{ab} = \left(\partial_a\boldsymbol{h}|\partial_b\boldsymbol{h}\right) \tag{3.68}$$

is the Fisher information matrix. We see that it controls the variance of likelihood distribution.

The form of the posterior distribution we depend upon the nature of the prior information. If we have an uninformative prior, such that $p(\boldsymbol{\lambda})$ is a constant, then

the posterior distribution would be determined by the likelihood. In the high SNR limit, we would obtain a Gaussian with variance-covariance matrix

$$\boldsymbol{\Sigma} = \boldsymbol{\Gamma}^{-1}. \tag{3.69}$$

The Fisher information matrix gives the uncertainty associated with the estimated parameter values, in this case the maximum-likelihood values. If the prior were to restrict the allowed range of parameters, for example we believe that the spin parameter is $|a| \leq M_\bullet$, then the posterior would be a truncated Gaussian, and $\boldsymbol{\Gamma}^{-1}$ would no longer represent the variance-covariance. If the prior was approximately Gaussian with variance-covariance matrix $\boldsymbol{\Sigma}_0$, then the posterior would also be Gaussian.[6] The posterior variance-covariance would be[39, 44]

$$\boldsymbol{\Sigma} = \left(\boldsymbol{\Gamma} + \boldsymbol{\Sigma}_0^{-1}\right)^{-1}. \tag{3.70}$$

As a first estimate of what we may learn from parabolic encounters we have only looked at the Fisher information matrix elements. If these are large then we expect we would be able to precisely determine a parameter, whereas if they are small we would not be able to learn much more than we already know from our prior knowledge. The input parameters for the model are:

3.7 Energy Spectra

We may compare the energy spectrum calculated from the kludge waveform with that obtain from the classic treatment of Peters and Matthews[45, 46]. These calculate GW emission for Keplerian orbits in flat spacetime, assuming only quadrupole radiation. The spectrum produced should be similar to that obtained from the NK in weak fields, that is for orbits with a large periapsis, however we do not expect an exact match because of the differing input physics and various approximations.

3.7.1 Kludge Spectrum

Our gravitational wave in the TT gauge has momentum pseudotensor[5]

$$T_{\mu\nu} = \frac{c^4}{32\pi G}\left\langle \partial_\mu h_{ij} \partial_\nu h^{ij} \right\rangle, \tag{3.71}$$

where $\langle \ldots \rangle$ indicates averaging over several wavelengths, or equivalently averaging over several periods. Thus, the flux of energy through a sphere of radius $r = R$ is

$$\frac{\mathrm{d}E}{\mathrm{d}t} = \frac{c^3}{32\pi G} R^2 \int \mathrm{d}\Omega \left\langle \frac{\mathrm{d}h_{ij}}{\mathrm{d}t} \frac{\mathrm{d}h^{ij}}{\mathrm{d}t} \right\rangle, \tag{3.72}$$

[6] If we only know the typical value and spread of a parameter then a Gaussian is the maximum entropy prior[43]: the prior that is least informative given what we do know, the prior that best reflects our state of ignorance.

with $\int \mathrm{d}\Omega$ representing integration over all solid angles. From equation (3.27) we see that the waves have a $1/r$ dependence, so if we define

$$h_{ij} = \frac{H_{ij}}{r}, \tag{3.73}$$

we see that the flux is independent of R, as required for energy conservation,

$$\frac{\mathrm{d}E}{\mathrm{d}t} = \frac{c^3}{32\pi G} \int \mathrm{d}\Omega \left\langle \frac{\mathrm{d}H_{ij}}{\mathrm{d}t} \frac{\mathrm{d}H^{ij}}{\mathrm{d}t} \right\rangle. \tag{3.74}$$

If we now integrate to find the total energy emitted we obtain

$$E = \frac{c^3}{32\pi G} \int \mathrm{d}\Omega \int_{-\infty}^{\infty} \mathrm{d}t \frac{\mathrm{d}H_{ij}}{\mathrm{d}t} \frac{\mathrm{d}H^{ij}}{\mathrm{d}t}. \tag{3.75}$$

Since we are considering all times the localization of the energy is no longer of importance and so it is unnecessary to average over several periods. If we switch to Fourier representation $\widetilde{H}_{ij}(f) = \mathscr{F}\{H_{ij}(t)\}$, then

$$\begin{aligned} E &= \frac{c^3}{32\pi G} \int \mathrm{d}\Omega \int_{-\infty}^{\infty} \mathrm{d}t \int_{-\infty}^{\infty} \mathrm{d}f 2\pi i f \widetilde{H}_{ij}(f) e^{2\pi i f t} \int_{-\infty}^{\infty} \mathrm{d}f' 2\pi i f' \widetilde{H}^{ij}(f') e^{2\pi i f' t} \\ &= \frac{\pi c^3}{8G} \int \mathrm{d}\Omega \int_{-\infty}^{\infty} \mathrm{d}f f^2 \widetilde{H}_{ij}(f) \widetilde{H}^{ij}(-f) \\ &= \frac{\pi c^3}{4G} \int \mathrm{d}\Omega \int_{0}^{\infty} \mathrm{d}f f^2 \widetilde{H}^{ij}(f) \widetilde{H}^{*}_{ij}(f). \end{aligned} \tag{3.76}$$

Here we have used that the signal is real so that $\widetilde{H}^{*}_{ij}(f) = \widetilde{H}_{ij}(-f)$. Using this we can identify the energy spectrum as

$$\frac{\mathrm{d}E}{\mathrm{d}f} = \frac{\pi c^3}{4G} \int \mathrm{d}\Omega f^2 \widetilde{H}^{ij}(f) \widetilde{H}^{*}_{ij}(f). \tag{3.77}$$

3.7.2 Peters & Matthews Spectrum

To calculate the energy spectrum for a parabolic orbit, we follow the derivation of Gair[47]. Peters and Matthews give the power radiated into the nth harmonic of the orbital angular frequency as

$$P(n) = \frac{32}{5} \frac{G^4}{c^5} \frac{M_\bullet^2 \mu^2 (M_\bullet + \mu)(1-e)^5}{{r_p}^5} g(n,e) \tag{3.78}$$

where the function $g(n,e)$ is defined in terms of Bessel functions of the first kind

$$\begin{aligned} g(n,e) = \frac{n^4}{32} \Bigg\{ &\Big[J_{n-2}(ne) - 2e J_{n-1}(ne) + \frac{2}{n} J_n(ne) + 2e J_{n+1}(ne) - J_{n+2}(ne) \Big]^2 \\ &+ \left(1 - e^2\right) \left[J_{n-2}(ne) - 2 J_n(ne) + J_{n+2}(ne) \right]^2 + \frac{4}{3n^2} \left[J_n(ne) \right]^2 \Bigg\}. \end{aligned} \tag{3.79}$$

The Keplerian orbital frequency is

$$\omega_0{}^2 = \frac{G(M_\bullet + \mu)(1-e)^3}{r_p{}^3} \tag{3.80}$$

$$= (1-e)^3 \omega_{\rm c}{}^2, \tag{3.81}$$

where $\omega_{\rm c}$ is defined as the orbital angular frequency of a circular orbit of radius equal to r_p. The total energy radiated into the nth harmonic, that is at frequency $\omega_n = n\omega_0$, is the power multiplied by the orbital period

$$E(n) = \frac{2\pi}{\omega_0} P(n); \tag{3.82}$$

as $e \to 1$ for a parabolic orbit, $\omega_0 \to 0$ so the orbital period becomes infinite. We may therefore identify the energy radiated per orbit with the total orbital energy radiated. Since the spacing of harmonics is $\Delta\omega = \omega_0$, we may identify the energy spectrum

$$\left.\frac{{\rm d}E}{{\rm d}\omega}\right|_{\omega_n} \omega_0 = E(n). \tag{3.83}$$

Using the above relations, and changing to linear frequency $2\pi f = \omega$, we obtain

$$\left.\frac{{\rm d}E}{{\rm d}f}\right|_{f_n} = \frac{128\pi^2}{5}\frac{G^3}{c^5}\frac{M_\bullet^2\mu^2}{r_p^2}(1-e)^2 g(n,e) \tag{3.84}$$

$$= \frac{4\pi^2}{5}\frac{G^3}{c^5}\frac{M_\bullet^2\mu^2}{r_p^2}\ell(n,e), \tag{3.85}$$

where we have defined the function $\ell(n,e)$ in the last line. For a parabolic orbit, we now have to take the limit of $\ell(n,e)$ as $e \to 1$.

We shall simplify $\ell(n,e)$ using the recurrence formulae[48]

$$J_{\nu-1}(z) + J_{\nu+1}(z) = \frac{2\nu}{z} J_\nu(z) \tag{3.86}$$

$$J_{\nu-1}(z) - J_{\nu+1}(z) = 2J'_\nu(z). \tag{3.87}$$

We shall also eliminate n using

$$n = \frac{\omega_n}{\omega_0}$$

$$= (1-e)^{-3/2}\widetilde{f}. \tag{3.88}$$

where $\widetilde{f} = \omega_n/\omega_{\rm c} = f_n/f_{\rm c}$ is a dimensionless frequency. We begin by breaking ℓ into three parts

$$\ell = \underbrace{(1-e)^2 n^4 \left[J_{n-2} - 2eJ_{n-1} + \frac{2}{n}J_n + 2eJ_{n+1} - J_{n+2}\right]^2}_{\ell_1}$$

$$+ \underbrace{(1-e)^3(1+e)n^4\left[J_{n-2} - 2J_n + J_{n+2}\right]^2}_{\ell_2} + \underbrace{\frac{4(1-e)^2 n^2}{3}\left[J_n\right]^2}_{\ell_3}. \tag{3.89}$$

We have suppressed the argument of the Bessel functions for brevity. Tackling each term of ℓ in turn we obtain

$$\ell_1(\widetilde{f},e) = \left[\frac{4(1+e)\widetilde{f}^2}{e}\frac{J_n'}{1-e} + 2\frac{e-2}{e}\widetilde{f}\frac{J_n}{(1-e)^{1/2}}\right]^2 \tag{3.90}$$

$$\ell_2(\widetilde{f},e) = 16(1+e)\left[\frac{(1+e)\widetilde{f}^2}{e^2}\frac{J_n}{(1-e)^{1/2}} - \widetilde{f}\frac{J_n'}{e}\right]^2 \tag{3.91}$$

$$\ell_3(\widetilde{f},e) = \frac{4\widetilde{f}^2}{3}\left[J_n(1-e)^{1/2}\right]^2. \tag{3.92}$$

To take the limit of these we need to find the limiting behaviour of Bessel functions. We shall define two new functions

$$A(\widetilde{f}) = \lim_{e\to 1}\left\{\frac{J_n}{(1-e)^{1/2}}\right\}; \quad B(\widetilde{f}) = \lim_{e\to 1}\left\{\frac{J_n'}{1-e}\right\}. \tag{3.93}$$

To give a well defined energy spectrum, both of these must be finite. In this case we see that the second term in ℓ_2 should go to zero.

The Bessel function has an integral representation [48]

$$J_\nu(z) = \frac{1}{\pi}\int_0^\pi \cos(\nu\theta - z\sin\theta)\,\mathrm{d}\theta, \tag{3.94}$$

we want the limit of this for $\nu\to\infty$, $z\to\infty$, with $z\leq\nu$. We will use the stationary phase approximation to argue that the predominant contribution to the integral comes from when the argument of the cosine is approximately zero, that is for small θ. In this case we have [48]

$$J_\nu(z) \sim \frac{1}{\pi}\int_0^\pi \cos\left(\nu\theta - z\theta + \frac{z}{6}\theta^3\right)\mathrm{d}\theta \tag{3.95}$$

$$\sim \frac{1}{\pi}\int_0^\infty \cos\left(\nu\theta - z\theta + \frac{z}{6}\theta^3\right)\mathrm{d}\theta; \tag{3.96}$$

this last expression is an Airy integral. The Airy integral has a standard from [48]

$$\int_0^\infty \cos(t^3+xt)\,\mathrm{d}t = \frac{\sqrt{x}}{3}K_{1/3}\left(\frac{2x^{3/2}}{3^{3/2}}\right), \tag{3.97}$$

where $K_\nu(z)$ is a modified Bessel function of the second kind. Using this to evaluate our limit gives

$$J_\nu(z) \sim \frac{1}{\pi}\sqrt{\frac{2(\nu-z)}{3z}}K_{1/3}\left(\frac{2^{3/2}}{3}\sqrt{\frac{(\nu-z)^3}{z}}\right). \tag{3.98}$$

For our particular case we have

$$\nu = (1-e)^{-3/2}\widetilde{f}; \quad z = (1-e)^{-3/2}e\widetilde{f}; \tag{3.99}$$

$$\frac{\nu-z}{z} = (1-e); \quad \frac{(\nu-z)^3}{z} = \widetilde{f}^2; \tag{3.100}$$

so we find

$$J_n(ne) \sim \frac{1}{\pi}\sqrt{\frac{2}{3}}(1-e)^{1/2}K_{1/3}\left(\frac{2^{3/2}\widetilde{f}}{3}\right), \tag{3.101}$$

thus

$$A(\widetilde{f}) = \frac{1}{\pi}\sqrt{\frac{2}{3}}K_{1/3}\left(\frac{2^{3/2}\widetilde{f}}{3}\right) \tag{3.102}$$

is well defined.

Now finding the derivative

$$\begin{aligned} J'_\nu(z) &= \frac{1}{2}\left[J_{\nu-1}(z) - J_{\nu+1}(z)\right] \\ &\sim \frac{1}{2\pi}\left[\sqrt{\frac{2(\nu-1-z)}{3z}}K_{1/3}\left(\frac{2^{3/2}}{3}\sqrt{\frac{(\nu-1-z)^3}{z}}\right)\right. \\ &\quad \left. -\sqrt{\frac{2(\nu+1-z)}{3z}}K_{1/3}\left(\frac{2^{3/2}}{3}\sqrt{\frac{(\nu+1-z)^3}{z}}\right)\right]. \end{aligned} \tag{3.103}$$

For our case

$$\sqrt{\frac{\nu\pm1-z}{z}} = (1-e)^{1/2}\left[1 \pm \frac{(1-e)^{1/2}}{2\widetilde{f}} + \ldots\right]; \tag{3.104}$$

$$\sqrt{\frac{(\nu\pm1-z)^{3/2}}{z}} = \widetilde{f}\left[1 \pm \frac{3(1-e)^{1/2}}{2\widetilde{f}} + \ldots\right]; \tag{3.105}$$

and so

$$\begin{aligned} J'_n(ne) &\sim \frac{1}{2\pi}\sqrt{\frac{2}{3}}(1-e)^{1/2}\left\{\left[1-\frac{(1-e)^{1/2}}{2\widetilde{f}}\right]K_{1/3}\left(\frac{2^{3/2}\widetilde{f}}{3}\left[1-\frac{3(1-e)^{1/2}}{2\widetilde{f}}\right]\right)\right. \\ &\quad \left. -\left[1+\frac{(1-e)^{1/2}}{2\widetilde{f}}\right]K_{1/3}\left(\frac{2^{3/2}\widetilde{f}}{3}\left[1-\frac{3(1-e)^{1/2}}{2\widetilde{f}}\right]\right)\right] \\ &\sim \frac{-1}{2\pi}\sqrt{\frac{2}{3}}(1-e)\left[2^{3/2}K'_{1/3}\left(\frac{2^{3/2}\widetilde{f}}{3}\right) + \frac{1}{\widetilde{f}}K_{1/3}\left(\frac{2^{3/2}\widetilde{f}}{3}\right)\right]. \end{aligned} \tag{3.106}$$

We may re-express the derivative using the recurrence formula [48]

$$K_{\nu-1}(z) - K_{\nu+1}(z) = -2K'_\nu(z) \tag{3.107}$$

to give

$$J'_n(ne) \sim \frac{1-e}{\sqrt{3}\pi}\left[K_{-2/3}\left(\frac{2^{3/2}\widetilde{f}}{3}\right) + K_{4/3}\left(\frac{2^{3/2}\widetilde{f}}{3}\right) - \frac{1}{\sqrt{2}\widetilde{f}}K_{1/3}\left(\frac{2^{3/2}\widetilde{f}}{3}\right)\right]. \tag{3.108}$$

And so finally,

$$B(\widetilde{f}) = \frac{1}{\sqrt{3}\pi}\left[K_{-2/3}\left(\frac{2^{3/2}\widetilde{f}}{3}\right) + K_{4/3}\left(\frac{2^{3/2}\widetilde{f}}{3}\right) - \frac{1}{\sqrt{2}\widetilde{f}}K_{1/3}\left(\frac{2^{3/2}\widetilde{f}}{3}\right)\right], \tag{3.109}$$

which is also well defined.

Having obtained expressions for $A(\widetilde{f})$ and $B(\widetilde{f})$ in terms of standard functions, we may now calculate the energy spectrum for a parabolic orbit. From equation (3.85) we have

$$\frac{\mathrm{d}E}{\mathrm{d}f} = \frac{4\pi^2}{5}\frac{G^3}{c^5}\frac{M_\bullet^2\mu^2}{r_p^2}\ell\left(\frac{f}{f_\mathrm{c}}\right), \tag{3.110}$$

where we have used the limit

$$\begin{aligned}\ell(\widetilde{f}) &= \lim_{e\to 1}\{\ell(n,e)\}\\ &= \left[8\widetilde{f}B(\widetilde{f}) - 2\widetilde{f}A(\widetilde{f})\right]^2 + \left(128\widetilde{f}^4 + \frac{4\widetilde{f}^2}{3}\right)\left[A(\widetilde{f})\right]^2.\end{aligned} \tag{3.111}$$

To check the validity of this limit we may calculate the total energy radiated. We should be able to calculate this by integrating equation (3.110) over all frequencies, or alternatively by summing the energy radiated into each harmonic. For consistency, the two approaches should yield the same result. First, summing over harmonics the

$$\begin{aligned}E_\mathrm{sum} &= \sum_n E(n)\\ &= \frac{64\pi}{5}\frac{G^3}{c^5}\frac{M_\bullet^2\mu^2}{r_p^2}\omega_\mathrm{c}(1-e)^{7/2}\sum_n g(n,e),\end{aligned} \tag{3.112}$$

where we have used equations (3.78), (3.81) and (3.82). Peters and Matthews[45] provide the result

$$\sum_n g(n,e) = \frac{1 + {}^{73}\!/_{24}\,e^2 + {}^{37}\!/_{96}\,e^4}{(1-e^2)^{7/2}}. \tag{3.113}$$

Using this,

$$E_\mathrm{sum} = \frac{64\pi}{5}\frac{G^3}{c^5}\frac{M_\bullet^2\mu^2}{r_p^2}\omega_\mathrm{c}\frac{1 + {}^{73}\!/_{24}\,e^2 + {}^{37}\!/_{96}\,e^4}{(1+e^2)^{7/2}}. \tag{3.114}$$

This is perfectly well behaved as $e \to 1$. Taking the limit for a parabolic orbit, the total energy radiated is

$$E_\mathrm{sum} = \frac{85\pi}{2^{5/2}3}\frac{G^3}{c^5}\frac{M_\bullet^2\mu^2}{r_p^2}\omega_\mathrm{c}. \tag{3.115}$$

Integrating over the energy spectrum, equation (3.110), gives

$$\begin{aligned}E_\mathrm{int} &= \int_0^\infty \frac{\mathrm{d}E}{\mathrm{d}f}\,\mathrm{d}f\\ &= \frac{2\pi}{5}\frac{G^3}{c^5}\frac{M_\bullet^2\mu^2}{r_p^2}\omega_\mathrm{c}\int_0^\infty \ell(\widetilde{f})\,\mathrm{d}\widetilde{f}.\end{aligned} \tag{3.116}$$

The integral can be easily evaluated numerically showing

$$\begin{aligned}\int_0^\infty \ell(\widetilde{f})\,\mathrm{d}\widetilde{f} &= 12.5216858\ldots\\ &= \frac{425}{2^{7/2}3},\end{aligned} \tag{3.117}$$

and so we find that the two total energies are consistent

$$E_{\rm int} = \frac{85\pi}{2^{5/2}3}\frac{G^3}{c^5}\frac{M_\bullet^2\mu^2}{r_p^2}\omega_{\rm c} \tag{3.118}$$

$$= E_{\rm sum}. \tag{3.119}$$

3.7.3 Comparison

The total energy flux from the kludge waveform is larger than the Peters and Matthews result. This behaviour has been seen before for high eccentricity orbits about a non-spinning BH[32].

3.8 Discussion & Further Work

Chapter 4

Future Work

Bibliography

[1] Landau, L. D. & Lifshitz, E. M.; *The Classical Theory of Fields*; fourth edition; Course of Theoretical Physics; Oxford: Butterworth-Heinemann, 1975.

[2] Will, C. M.; The Confrontation between General Relativity and Experiment; *Living Reviews in Relativity*; **9**(3), 2006.

[3] Sotiriou, T. P. & Faraoni, V.; $f(R)$ theories of gravity; *Reviews of Modern Physics*; **82**(1):451–497, March 2010.

[4] De Felice, A. & Tsujikawa, S.; $f(R)$ theories; *Living Reviews in Relativity*; **13**(3), February 2010.

[5] Misner, C. W., Thorne, K. S. & Wheeler, J. A.; *Gravitation*; New York: W. H. Freeman, 1973.

[6] Buchdahl, H. A.; Non-linear Lagrangians and cosmological theory; *Monthly Notices of the Royal Astronomical Society*; **150**:1–8, 1970.

[7] Psaltis, D., Perrodin, D., Dienes, K. R. & Mocioiu, I.; Kerr Black Holes Are Not Unique to General Relativity; *Physical Review Letters*; **100**(9):091101(4), March 2008.

[8] Exirifard, Q. & Sheik-Jabbari, M.; Lovelock gravity at the crossroads of Palatini and metric formulations; *Physics Letters B*; **661**(2-3):158–161, March 2008.

[9] Lynden-Bell, D. & Rees, M. J.; On quasars, dust and the galactic centre; *Monthly Notices of the Royal Astronomical Society*; **152**, 1971.

[10] Rees, M. J.; Black Hole Models for Active Galactic Nuclei; *Annual Review of Astronomy and Astrophysics*; **22**(1):471–506, September 1984.

[11] Israel, W.; Event Horizons in Static Vacuum Space-Times; *Physical Review*; **164**(5):1776–1779, December 1967.

[12] Israel, W.; Event horizons in static electrovac space-times; *Communications in Mathematical Physics*; **8**(3):245–260, September 1968.

[13] Carter, B.; Axisymmetric Black Hole Has Only Two Degrees of Freedom; *Physical Review Letters*; **26**(6):331–333, February 1971.

[14] Hawking, S. W.; Black holes in general relativity; *Communications in Mathematical Physics*; **25**(2):152–166, June 1972.

[15] Robinson, D.; Uniqueness of the Kerr Black Hole; *Physical Review Letters*; **34**(14):905–906, April 1975.

[16] Chandrasekhar, S.; *The Mathematical Theory of Black Holes*; Oxford Classic Texts in the Physical Sciences; Oxford: Oxford University Press, 1998.

[17] Merritt, D., Mikkola, S. & Will, C. M.; Testing properties of the Galactic center black hole using stellar orbits; *Physical Review D*; **81**(6):062002(17), March 2010.

[18] Kato, Y., Miyoshi, M., Takahashi, R. *et al.*; Measuring spin of a supermassive black hole at the Galactic centre - implications for a unique spin; *Monthly Notices of the Royal Astronomical Society: Letters*; **403**(1):L74–L78, March 2010.

[19] Bender, P., Brillet, A., Ciufolini, I. *et al.*; LISA Pre-Phase A Report, 1998.

[20] Danzmann, K. & R\"{u}diger, A.; LISA technology concept, status, prospects; *Classical and Quantum Gravity*; **20**(10):S1–S9, May 2003.

[21] Rubbo, L. J., Holley-Bockelmann, K. & Finn, L. S.; *Event Rate for Extreme Mass Ratio Burst Signals in the LISA Band*; AIP, 2006; URL `http://arxiv.org/abs/astro-ph/0602445`.

[22] Kobayashi, S., Laguna, P., Phinney, E. S. & Meszaros, P.; Gravitational Waves and X-Ray Signals from Stellar Disruption by a Massive Black Hole; *The Astrophysical Journal*; **615**(2):855–865, November 2004.

[23] Babak, S., Fang, H., Gair, J. *et al.*; "Kludge" gravitational waveforms for a test-body orbiting a Kerr black hole; *Physical Review D*; **75**(2):024005(25), January 2007.

[24] Kerr, R.; Gravitational Field of a Spinning Mass as an Example of Algebraically Special Metrics; *Physical Review Letters*; **11**(5):237–238, September 1963.

[25] Boyer, R. H. & Lindquist, R. W.; Maximal Analytic Extension of the Kerr Metric; *Journal of Mathematical Physics*; **8**(2):265–281, February 1967.

[26] Hobson, M. P., Efstathiou, G. & Lasenby, A.; *General Relativity: An Introduction for Physicists*; Cambridge: Cambridge University Press, 2006.

[27] Carter, B.; Global Structure of the Kerr Family of Gravitational Fields; *Physical Review*; **174**(5):1559–1571, October 1968.

[28] de Felice, F.; Angular momentum and separation constant in the Kerr metric ; *Journal of Physics A: Mathematical and General*; **13**(5):1701–1708, 1980.

[29] Rosquist, K., Bylund, T. & Samuelsson, L.; Carter's Constant Revealed; *International Journal of Modern Physics D*; **18**(03):429–434, October 2009.

[30] Wilkins, D.; Bound Geodesics in the Kerr Metric; *Physical Review D*; **5**(4):814–822, February 1972.

[31] Drasco, S. & Hughes, S.; Rotating black hole orbit functionals in the frequency domain; *Physical Review D*; **69**(4):044015(11), February 2004.

[32] Gair, J., Kennefick, D. & Larson, S.; Semirelativistic approximation to gravitational radiation from encounters with nonspinning black holes; *Physical Review D*; **72**(8):084009(20), October 2005.

[33] Glampedakis, K. & Kennefick, D.; Zoom and whirl: Eccentric equatorial orbits around spinning black holes and their evolution under gravitational radiation reaction; *Physical Review D*; **66**(4):044002(33), August 2002.

[34] Ruffini, R. & Sasaki, M.; On a Semi-Relativistic Treatment of the Gravitational Radiation from a Mass Thrusted into a Black Hole; *Progress of Theoretical Physics*; **66**(5):1627–1638, November 1981.

[35] Press, W.; Gravitational radiation from sources which extend into their own wave zone; *Physical Review D*; **15**(4):965–968, February 1977.

[36] Bekenstein, J. D.; Gravitational-Radiation Recoil and Runaway Black Holes; *The Astrophysical Journal*; **183**:657, July 1973.

[37] Cutler, C.; Angular resolution of the LISA gravitational wave detector; *Physical Review D*; **57**(12):7089–7102, June 1998.

[38] Finn, L. S.; Detection, measurement, and gravitational radiation; *Physical Review D*; **46**(12):5236–5249, December 1992.

[39] Cutler, C., Kennefick, D. & Poisson, E.; Gravitational radiation reaction for bound motion around a Schwarzschild black hole; *Physical Review D*; **50**(6):3816–3835, September 1994.

[40] Barack, L. & Cutler, C.; LISA capture sources: Approximate waveforms, signal-to-noise ratios, and parameter estimation accuracy; *Physical Review D*; **69**(8):082005(24), April 2004.

[41] Jones, N. B. (editor); *Digital Signal Processing*; IEE Control Engineering Series; Exeter: Peter Peregrinus, 1982.

[42] Burko, L. M. & Khanna, G.; Accurate time-domain gravitational waveforms for extreme-mass-ratio binaries; *Europhysics Letters (EPL)*; **78**(6):60005, June 2007.

[43] Jaynes, E. T.; *Probability Theory: The Logic of Science*; Cambridge: Cambridge University Press, 2003.

[44] Vallisneri, M.; Use and abuse of the Fisher information matrix in the assessment of gravitational-wave parameter-estimation prospects; *Physical Review D*; **77**(4):042001(20), February 2008.

[45] Peters, P. C. & Mathews, J.; Gravitational Radiation from Point Masses in a Keplerian Orbit; *Physical Review*; **131**(1):435–440, July 1963.

[46] Peters, P. C.; Gravitational Radiation and the Motion of Two Point Masses; *Physical Review*; **136**(4B):B1224–B1232, November 1964.

[47] Gair, J. R.; private communication, 2010.

[48] Watson, G. N.; *A Treatise on the Theory of Bessel Functions*; second edition; Cambridge Mathematical Library; Cambridge: Cambridge University Press, 1995.